



Universiteit
Leiden
The Netherlands

Chemical tools to study the cannabinoid receptor type 2

Soethoudt, M.

Citation

Soethoudt, M. (2018, April 26). *Chemical tools to study the cannabinoid receptor type 2*. Retrieved from <https://hdl.handle.net/1887/62061>

Version: Not Applicable (or Unknown)

License: [Licence agreement concerning inclusion of doctoral thesis in the Institutional Repository of the University of Leiden](#)

Downloaded from: <https://hdl.handle.net/1887/62061>

Note: To cite this publication please use the final published version (if applicable).

Cover Page



Universiteit Leiden



The handle <http://hdl.handle.net/1887/62061> holds various files of this Leiden University dissertation

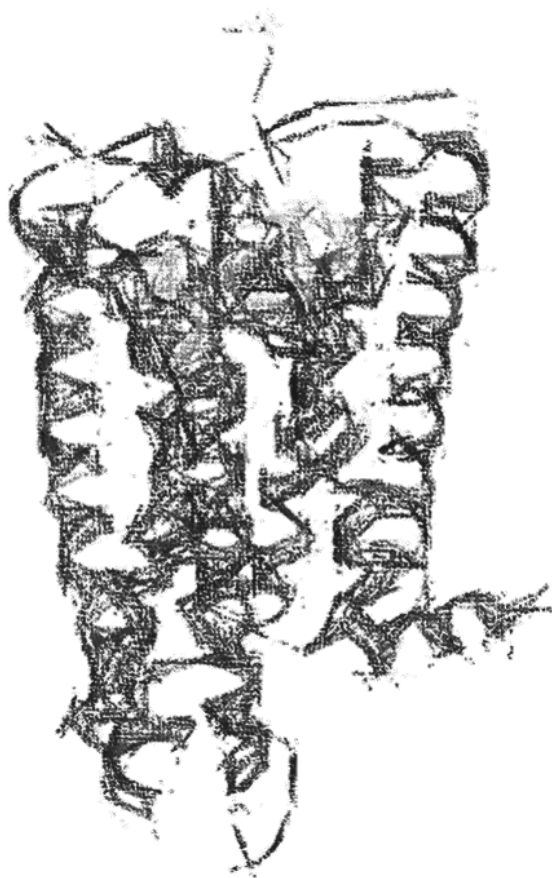
Author: Soethoudt, Marjolein

Title: Chemical tools to study the cannabinoid receptor type 2

Date: 2018-04-26

Chapter 5

Structure-Kinetic Relationship Studies of Cannabinoid Receptor Type 2 Agonists Reveal Substituent-Specific Lipophilic Effects on Residence Time¹



5.1 Introduction

Traditionally, in drug discovery, the affinity or potency of a drug candidate for a given target was considered a key determinant for *in vivo* activity (**Chapter 1**), but later it was found that these parameters do not correlate as well as originally thought.^{2,3} In contrast, the binding kinetics of a ligand for a given target, in particular slow dissociation kinetics and therefore a long target residence time, may be a better predictor of *in vivo* efficacy in specific cases,⁴⁻⁷ as emphasized by several excellent reviews.⁸⁻¹⁰ For example, a correlation was found between long residence time of Fab-I enoyl reductase inhibitors and their *in vivo* activity in a mouse model of tularemia infection, leading to prolonged survival of the mice.^{4, 5} Recently, this “drug-target residence time model” has aided several clinical-stage drug development programs^{11, 12} by selecting compounds with high efficacy,¹³ or reduced on-target toxicities.¹⁴ However, the association rate is increasingly recognized as well as an important factor in determining a ligand’s functional activity. For example, slowly associating ligands may decrease on-target related side effects by preventing high target occupancy and fast target activation,¹⁵ while fast associating ligands may have an influence in prolonged activity if rebinding occurs.¹⁶

Retrospective analysis of marketed drugs for G protein-coupled receptors (GPCRs), an important class of drug targets, revealed that the beneficial effects of some of these drugs may be attributed to their long drug-target residence times.⁹ Interestingly, in case of GPCR agonists, a positive correlation was also found between long residence time and *in vitro* efficacy for the Adenosine A_{2A} receptor¹⁷ and the Muscarinic M₃ receptor.¹⁸ For the latter, it was also shown that long target residence time of an antagonist, i.e. tiotropium, resulted in so-called kinetic selectivity over the other muscarinic receptor subtypes, thereby reducing off-target side effects.¹⁹

The cannabinoid CB₁ and CB₂ receptor (CB₁R and CB₂R) are class A GPCRs and both part of the endocannabinoid system. This signaling system comprises the receptors as well as their endogenous ligands, anandamide (AEA) and 2-arachidoylglycerol (2-AG), which are called endocannabinoids.²⁰ The CB₁R is mainly found within the central nervous system,²¹ which is therefore mainly responsible for the psycho-active effects of Δ^9 -tetrahydrocannabinol (THC), the main active substituent in cannabis.²² In contrast, the CB₂R is predominantly abundant in immune cells, is involved in cell migration and immunosuppression,^{23,24} and is upregulated during pathophysiological conditions.²⁵ CB₂R activity has been associated with therapeutic benefits in inflammatory or immune system related pathologies.^{25,26} Selective activation of the CB₂R is therefore associated with therapeutic benefits and may prevent CB₁R-mediated adverse side effects.

Recently, 3-cyclopropyl-1-(4-(6-((1,1-dioxidothiomorpholino)methyl)-5-fluoropyridin-2-yl)benzyl)imidazoleidine-2,4-dione (**LEI101**) (**Figure 1A**) was reported, a promising CB₂R partial agonist.²⁷ LEI101 showed *in vivo* efficacy in preclinical models of neuropathic pain and *cis*-platin-induced nephrotoxicity.^{27,28}

The CB₂R kinetic profile of LEI101 is unknown, therefore the binding kinetics and functional activity of this chemical series was systematically investigated. To this end, a library of 24 compounds was synthesized based on the scaffold of LEI101 (**Figure 1B**), in which their basicity and lipophilicity (pK_a and LogP) of the R¹ (amine) and R² (alkyl) substituents were systematically varied. From all agonists, the equilibrium binding affinity and Kinetic Rate Index (KRI), a high-throughput measure as an indication for ligand-receptor kinetics was determined.²⁹ In addition, the full kinetic profile, as well as functional potency and efficacy in G protein activation and β -arrestin recruitment, was measured for 14 of these compounds. Correlation analysis of the data identified a relationship between target residence time and potency in both signal transduction pathways due to increased lipophilicity specifically on the R² position. This work provides important insights in the impact of divergent binding kinetics of LEI101-based agonists on CB₂R pharmacology and the role of physicochemical properties therein. In turn, these insights show how CB₂R agonists can be designed to have optimal kinetic profiles, which will aid the lead optimization process in drug discovery for the study or treatment of inflammatory diseases.

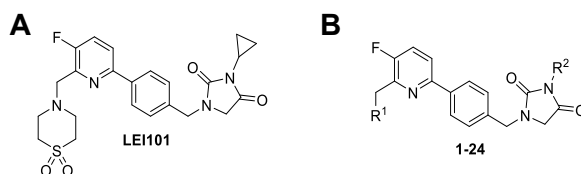
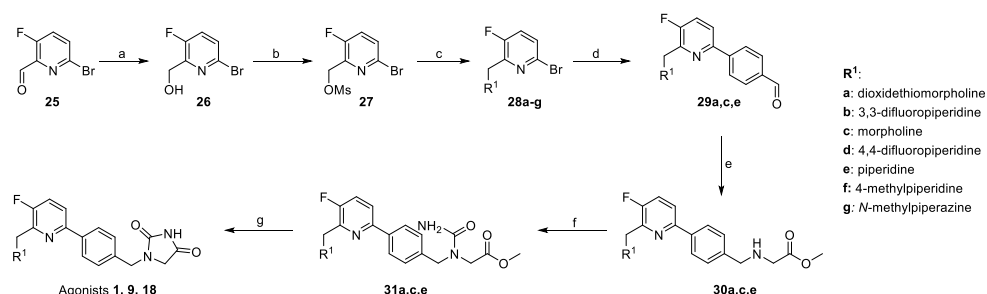


Figure 1. Chemical structures of LEI101 and the LEI101-based library of agonists (1-24) synthesized in this study.

5.2 Results

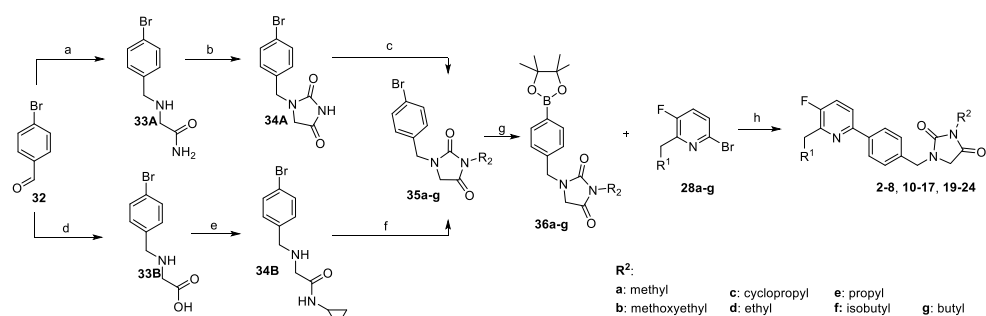
5.2.1 Synthesis of LEI101-based library

Starting from commercially available pyridinaldehyde **25**, the R¹ substituents were introduced in three steps (**Scheme 1**). First, the aldehyde was reduced with NaBH₄ in quantitative yield to its primary alcohol, which was then mesylated to enable nucleophilic substitution by the corresponding secondary amines of the R₁ substituents to yield intermediates **28a-g**. From here, compounds with R² = H were synthesized in four steps, starting with a Suzuki coupling with (4-formylphenyl)boronic acid, yielding aldehydes **29a,c,e** in excellent yield, which were subsequently used for reductive amination with methyl glycinate, to obtain biaryl intermediates **30a,c,e**. Final compounds **1**, **9** and **18** were then obtained in two additional steps, first by reaction of the secondary amine with sodium to form isocyanates **31a,c,e**, followed by cyclization to the hydantoin using NaOMe.



Scheme 1. Synthetic route towards building blocks **28a-g and agonists **1, 9** and **18**.** Reagents and conditions: a) NaBH₄, DCM:MeOH (2:1), rt, 80 min, 99%; b) Et₃N, Ms-Cl, THF, 0°C, 45 min, 72%; c) R¹-H, K₂CO₃, ACN, 50°C, 49–95%; d) (4-formyl)boronic acid, Pd(PPh₃)₄, K₂CO₃, Toluene:EtOH (4:1, degassed), 50°C, overnight, 60%-quantitative; e) Methylglycinate, NaBH(OAc)₃, THF:MeOH (3:1), rt, overnight; f) NaOCN, AcOH, DCM:water (1:1), rt; g) NaOMe, MeOH, rt, overnight, 9–43% (over three steps).

Compounds with R² ≠ H were synthesized using intermediates **28a-g** and the intermediates containing the R² substituents (**36a-g**) according to published procedures (**Scheme 2**).²⁸ Intermediates **35a-b** and **35d-g** were synthesized in three steps from bromobenzaldehyde **32**. A reductive amination with glycineamide yielded **33a**, which was cyclized to the hydantoin **34a** using carbonyldiimidazole (CDI). The hydantoin was then functionalized with the R² substituents using alkylation with the corresponding R²-halide to intermediates **35a-b** and **35d-g**. The synthesis to intermediate **35c** started with a reductive amination with glycine, yielding **33b**. The cyclopropyl substituent was then introduced using a peptide coupling with cyclopropylamine, yielding **34b** in good yield, which was then converted to intermediate **35c** by cyclization with CDI. Intermediates **35a-g** were converted into pinacolesters **36a-g** by Miyaura borylation, which were subsequently coupled to intermediates **28a-g** with a Suzuki coupling, to obtain final compounds **2-8, 10-17** and **19-24**.



Scheme 2. Synthetic route towards intermediates **35a-g and agonists **2-8, 10-17** and **19-24**.** Reagents and conditions: a) NaOH, 2-aminoacetamide·HCl, NaBH₄, MeOH:water (5:1), rt, 26 hr, 79%; b) CDI, DMAP, ACN, 60°C, 48 hr, 48%; c) R²-halide, K₂CO₃, DMF, 50°C, 77%-quantitative; d) Glycine, NaOH, NaBH₄, MeOH:water (5.5:1), rt, 40 hr, 90%; e) i) Et₃N, Boc₂O, water, rt, overnight, ii) DMF (cat.), SOCl₂, DCM, rt, 3.5 hr, iii) Cyclopropylamine, DCM, 0°C, overnight, 97%; f) CDI, DMAP, ACN, 60°C, overnight, 94%; g) KOAc, bis(pinacolato)diboron, Pd(dppf)Cl₂, DMF, 75°C, overnight; h) Pd(PPh₃)₄, K₂CO₃, Toluene:EtOH (4:1, degassed), 75°C, overnight, 9–87%.

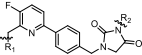
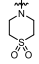
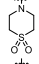

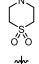
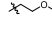
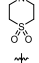
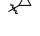
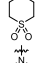

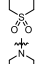

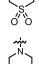

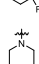

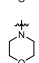
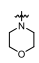
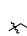
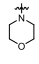
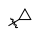
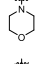

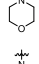

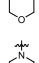

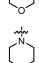

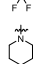

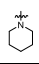

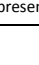


5.2.2 Equilibrium binding affinity of the LEI101-library

The affinities of the 24 newly synthesized compounds were determined in a radioligand displacement assay using [^3H]CP55940 as the radiolabeled competitor at a temperature of 25°C. The structure, affinity (pK_i) and physicochemical properties of the library are presented in **Table 1**. All compounds showed concentration-dependent displacement of [^3H]CP55940. Compounds **6**, **7**, **8**, **17**, **21**, **22** and **23**, carrying a propyl or isobutyl group at the R^2 position, displayed the highest affinities within the library ($\text{pK}_i > 7.5$). In contrast, compounds **3**, **11**, **16**, and **20**, carrying a more bulky methoxyethyl or butyl group at the R^2 position, displayed ~10- to 100-fold lower affinities, ranging from 5.35 ± 0.04 (compound **11**) to 6.56 ± 0.13 (compound **20**). Compounds **1**, **9** and **18**, without a substituent at R^2 , had the lowest affinities ($\text{pK}_i \approx 5.5$) of the library. On the R^1 position, compounds with a morpholine substituent (compounds **10-17**) or a piperazine (compound **24**) generally had lower affinities compared to corresponding dioxidethiomorpholino agonists with the same substituent at the R^2 position (e.g. compound **11** vs. **2** and **20**, **12** vs. **3** and **21** or **15** vs. **6** and **24**).

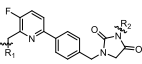
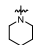
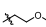
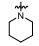
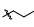
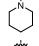
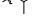
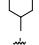

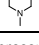
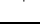
5.2.2 High throughput kinetic screening of LEI101-library

Next, the binding kinetics of all compounds were determined using the high throughput dual-point competition association assay, yielding Kinetic Rate Index (KRI) values that describe the relative (dissociation) kinetics of the agonist library compared to the radioligand used, [^3H]CP55940. These experiments, and all the following kinetic experiments, were performed at a reduced temperature of 10°C to increase the ‘resolution’ of the assay, enabling us to examine the influence of different physicochemical properties on the relative binding kinetics of the compounds within the library. Firstly, it was validated that the affinities of the molecules were similar (particularly in rank order) at 10°C as compared to 25°C using a selection of 8 representative agonists with low, moderate and high affinity (data not shown). Subsequently, a single concentration of the compounds was used ($1.0 \times \text{IC}_{50}$) for determination of the KRI values (**Table 1**). Most compounds had a KRI value lower than 1.0, which indicates a residence time (RT) shorter than that of [^3H]CP55940. Compounds **2**, **4** and **6** had the lowest KRI values (0.53 ± 0.06 , 0.52 ± 0.09 and 0.51 ± 0.05 , respectively), whereas only **7**, **22** and **23** had a KRI value larger than 1.0 (1.06 ± 0.11 , 1.21 ± 0.07 and 1.03 ± 0.08 , respectively). These three compounds all have an isobutyl moiety at the R^2 position, the most lipophilic substituent in this series, but have different R^1 substituents, a dioxidethiomorpholine (**7**), a piperidine (**22**), or a methylpiperidine (**23**).

Table 1. Overview of chemical structures, physicochemical properties, equilibrium affinity and Kinetic Rate Index (KRI) of the LEI101-based agonist library

			Physicochemical properties			Binding affinity	Kinetic Rate Index
Nr.	R ¹	R ²	MW (Da)	cLogP	pK _a	pK _i ± SEM	KRI ± SEM
1		H	432	0.4	5.1	5.55 ± 0.08	0.62 ± 0.06
2			447	0.4	5.1	6.61 ± 0.18	0.53 ± 0.06
3			491	0.8	5.1	6.25 ± 0.04	0.67 ± 0.03
4 LEI101			473	0.9	5.1	6.51 ± 0.09	0.52 ± 0.09
5			461	0.9	5.1	7.06 ± 0.12	0.51 ± 0.05
6			475	1.5	5.1	7.66 ± 0.08	0.71 ± 0.05
7			489	1.9	5.1	7.74 ± 0.08	1.06 ± 0.11
8			475	4.4	6.1	7.48 ± 0.10	0.79 ± 0.05
9		H	384	1.3	6.3	5.65 ± 0.05	0.72 ± 0.08
10			398	1.4	6.3	6.06 ± 0.24	0.71 ± 0.06
11			442	1.7	6.3	5.35 ± 0.04	0.77 ± 0.05
12			424	1.9	6.3	6.17 ± 0.03	0.67 ± 0.12
13			412	1.9	6.3	6.84 ± 0.25	0.71 ± 0.08
14			426	2.4	6.3	7.13 ± 0.15	0.57 ± 0.08
15			441	2.8	6.3	7.07 ± 0.10	0.67 ± 0.05
16			440	3.0	6.3	6.21 ± 0.20	0.62 ± 0.12
17			475	3.5	6.9	7.67 ± 0.14	0.85 ± 0.13
18		H	382	2.6	8.3	5.48 ± 0.06	0.68 ± 0.07
19			396	2.6	8.3	6.70 ± 0.05	0.60 ± 0.08

Values are presented as mean ± SEM (N=3, n=2); cLogP and pK_a were determined with Chemdraw Professional 16.0

			Physicochemical properties			Binding affinity	Kinetic Rate Index
Nr.	R ¹	R ²	MW (Da)	cLogP	pKa	pK _i ± SEM	KRI ± SEM
20			440	3.0	8.3	6.56 ± 0.13	0.78 ± 0.05
21			425	3.7	8.3	7.92 ± 0.06	0.66 ± 0.14
22			439	4.1	8.3	7.56 ± 0.02	1.21 ± 0.07
23			453	4.6	8.3	7.61 ± 0.22	1.03 ± 0.08
24			454	3.3	8.8	5.45 ± 0.09	0.67 ± 0.01

Values are presented as mean ± SEM (N=3, n=2); cLogP and pK_a were determined with Chemdraw Professional 16.0

5.2.3 Full kinetic profiling of the LEI101-library

Based on the results from the KRI screen, twelve agonists were selected for further kinetic characterization. These compounds contained a dioxidethiomorpholine at the R¹ position (group A, compounds **1-7**) or an isobutyl group at the R² position (group B, compounds **7, 8, 15, 17, 22, 23**). Of note, compound **7** belongs to both groups. The molecules comprised a wide range of KRI values between 0.51 and 1.21, respectively the lowest and highest KRI measured in this agonist library. Together this allowed a comprehensive investigation of structure-kinetic relationships at the CB₂R. A competition association assay with [³H]CP55940 was used that yielded the association- and dissociation rate constants (k_{on} and k_{off} values, respectively) of the compounds (Table 2).

Table 2. Overview of binding kinetics and functional activity in two signal transduction pathways.

Nr.	Group	Binding kinetics				Functional activity			
		k _{off} (s ⁻¹)	k _{on} (M ⁻¹ s ⁻¹)	K _D (nM)	RT (min)	G protein activation		β-arrestin recruitment	
						pEC ₅₀	E _{max}	pEC ₅₀	E _{max}
1	A	(2.7 ± 1.8) × 10 ⁻³	(2.2 ± 1.0) × 10 ³	1052 ± 264	14 ± 6	6.25 ± 0.09	48 ± 7	6.12 ± 0.23	25 ± 2
2	A	(1.2 ± 0.6) × 10 ⁻²	(1.0 ± 0.7) × 10 ⁵	155 ± 35	2.2 ± 0.8	6.18 ± 0.27	54 ± 13	6.55 ± 0.18	76 ± 15
3	A	(7.1 ± 3.3) × 10 ⁻³	(4.4 ± 2.6) × 10 ⁴	187 ± 25	3.6 ± 1.5	6.06 ± 0.27	60 ± 2	6.58 ± 0.08	45 ± 7
4 (LEI101)	A	(2.1 ± 0.5) × 10 ⁻³	(3.0 ± 1.1) × 10 ⁴	76 ± 10	8.8 ± 1.6	6.6 ± 0.2 ^f	65 ± 8 ^f	7.0 ± 0.3 ^f	41 ± 6 ^f
5	A	(1.5 ± 0.9) × 10 ⁻³	(5.3 ± 2.6) × 10 ⁴	26 ± 2	20 ± 8	6.38 ± 0.28	79 ± 14	6.76 ± 0.39	72 ± 10
6	A	(5.9 ± 1.3) × 10 ⁻⁴	(6.8 ± 1.7) × 10 ⁴	9 ± 2	32 ± 9	7.78 ± 0.07	50 ± 2	7.88 ± 0.10	62 ± 8
7	A/B	(2.4 ± 0.1) × 10 ⁻⁴	(5.3 ± 0.4) × 10 ⁴	4.5 ± 0.5	71 ± 3	7.94 ± 0.24	60 ± 6	7.83 ± 0.08	56 ± 1
8	B	(4.7 ± 0.1) × 10 ⁻⁴	(5.9 ± 1.6) × 10 ⁴	9 ± 1	37 ± 5	7.37 ± 0.07	61 ± 6	7.80 ± 0.07	54 ± 6
15	B	(4.3 ± 1.8) × 10 ⁻³	(1.9 ± 0.8) × 10 ⁵	24 ± 2	6.4 ± 2.9	7.18 ± 0.30	65 ± 12	7.21 ± 0.28	64 ± 10
17	B	(2.4 ± 0.3) × 10 ⁻⁴	(3.7 ± 1.0) × 10 ⁴	8 ± 2	72 ± 8	7.81 ± 0.15	65 ± 7	7.67 ± 0.03	53 ± 2
22	B	(2.4 ± 0.1) × 10 ⁻³	(2.3 ± 0.3) × 10 ⁴	11 ± 1	69 ± 2	6.91 ± 0.32	78 ± 9	8.14 ± 0.08	67 ± 7
23	B	(5.9 ± 1.3) × 10 ⁻⁴	(7.8 ± 2.1) × 10 ⁴	9 ± 2	31 ± 6	7.61 ± 0.36	77 ± 14	7.89 ± 0.21	59 ± 6

All values are presented as mean ± SEM (N=3, n=2); K_D values are calculated using the formula: K_D = k_{off}/k_{on}

A significant correlation between the KRI values and k_{off} values was found (**Figure 2A**). The association of [^3H]CP55940 alone and in presence of a fast dissociating compound (**2**; KRI = 0.53 ± 0.06) and a slow dissociating compound (**7**; KRI = 1.06 ± 0.11) is shown in **Figure 2B**.

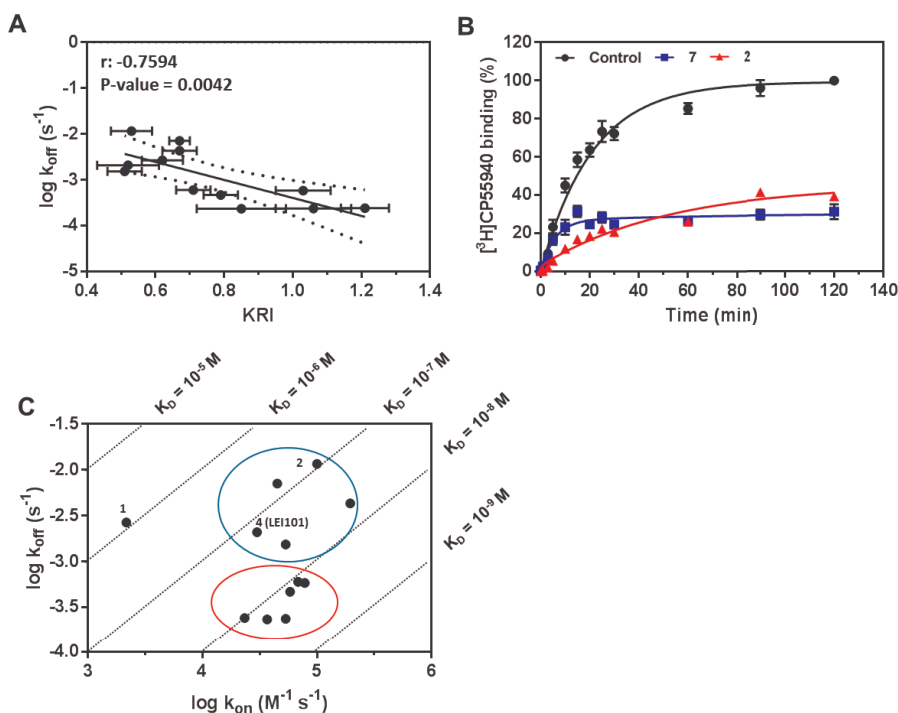


Figure 2: Kinetic characterization of the LEI101-agonist library. A) Correlation between KRI values and $\log k_{\text{off}}$ values. Correlation analysis was performed using a two-tailed Pearson correlation analysis (r = Pearson coefficient). B) Representative competition association curves from [^3H]CP55940 alone, or in presence with a long- (**7**) or short residence time (**2**) agonist. C) Kinetic map of $\log k_{\text{on}}$ vs $\log k_{\text{off}}$, where the diagonals represent the 'Kinetic' K_D value ($K_D = k_{\text{off}}/k_{\text{on}}$). A-C) Data with error is the mean and SEM of three independent experiments performed in duplicate and transformed data without error bars ($\log k_{\text{on}}$ and $\log k_{\text{off}}$) are derived from the mean of three independent experiments performed in duplicate.

The association of [^3H]CP55940 ($k_{\text{off}} = 1.9 \pm 0.1 \times 10^{-4} \text{ s}^{-1}$) in competition with **7** ($k_{\text{off}} = 2.4 \pm 0.1 \times 10^{-4} \text{ s}^{-1}$), resulted in a small overshoot after which it reached a plateau at $\sim 20\%$. In contrast, association of [^3H]CP55940 in competition with **2** ($k_{\text{off}} = 1.2 \pm 0.6 \times 10^{-2} \text{ s}^{-1}$) resulted in a gradual increase of [^3H]CP55940 binding over time. The k_{on} values varied between $2.2 \pm 1.0 \times 10^3 \text{ M}^{-1} \text{ s}^{-1}$ (**1**) and $1.9 \pm 0.8 \times 10^5 \text{ M}^{-1} \text{ s}^{-1}$ (**15**). Moreover, the variety in k_{on} and k_{off} values was visualized using a kinetic map (**Figure 2C**), created by plotting the k_{on} values against k_{off} values. The diagonals represent the 'kinetic' K_D value ($K_D = k_{\text{off}}/k_{\text{on}}$) and show that compounds with similar K_D values can have different combinations of k_{off} and k_{on} values. For example, **2** and **LEI101** (**4**) have a similar K_D value ($K_D = 10^{-7} \text{ M}$), but have a more than 0.5 log-difference both in k_{off} and k_{on} values.

Of note, compounds with a $K_D \leq 10^{-8}$ M (circled in red) all have dissociation rates slower than 10^{-3} s^{-1} , while compounds with a dissociation rate between 10^{-3} and 10^{-2} s^{-1} (circled in blue) predominantly had a K_D between 10^{-7} and 10^{-8} M, due to a small variety in their k_{on} values. Of note, **1** ($R^2 = H$) had a 10-fold smaller k_{on} value compared to the other compounds, thereby making it an outlier in the kinetic map (Figure 2C). The kinetic K_D values of all compounds (Table 2) were compared to the equilibrium affinities (K_i values) (Figure 3A). A statistically significant correlation was found between the negative logarithm of the kinetic K_D (10°C) and the equilibrium pK_i (25°C). Of note, the pK_D values were all 0.5 log unit (~ 3 -fold) higher than the pK_i values. A correlation between pK_i and k_{off} or residence time was also identified (Figure 3B,C), but not between pK_i and k_{on} values (Figure 3D).

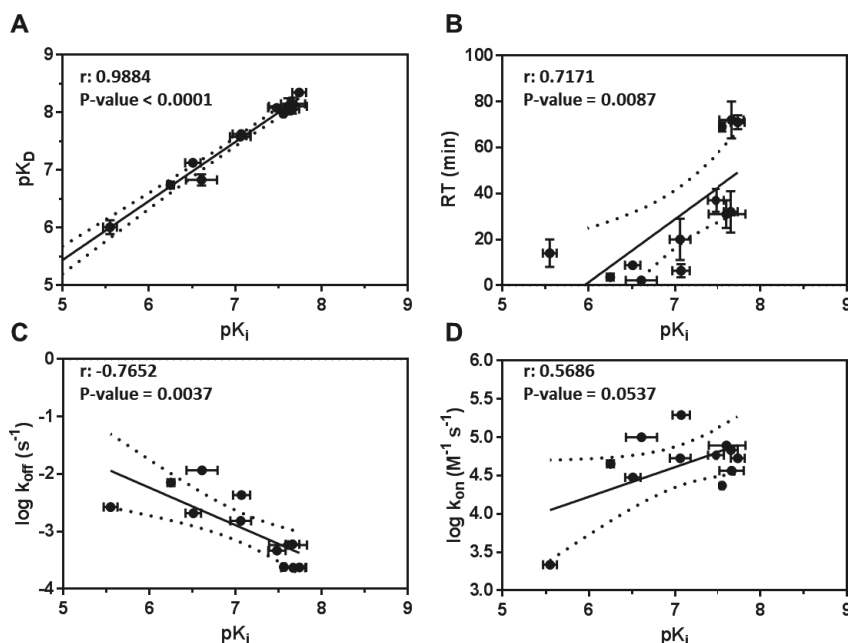


Figure 3. Comparison between equilibrium binding affinity and binding kinetics. A-D) Correlation plots of equilibrium affinity (pK_i) with the negative logarithmic transformation of kinetic affinity (pK_D) (A), residence time (RT) (B), dissociation rate k_{off} (C) and association rate k_{on} (D). All data with errors is the mean and SEM of three independent experiments performed in duplicate. Transformed data without error bars (K_D , $\log k_{on}$ and $\log k_{off}$) are derived from the mean of three independent experiments performed in duplicate. Correlation analysis was performed using a two-tailed Pearson correlation analysis (r = Pearson coefficient).

5.2.4 Structure-Kinetics Relationships

The kinetic profile of the compounds was used to derive structure-kinetics relationships. The longest residence times ($RT > 30$ min) were displayed by compounds with a propyl (**6**, $RT = 32 \pm 9$ min) or isobutyl group at the R^2 position (**7**, **8**, **17**, **22** and **23**, $RT = 71 \pm 3$, 37 ± 5 , 72 ± 8 , 69 ± 2 and 31 ± 6 min, respectively). Compounds **2** and **3** displayed the shortest residence times ($RT = 2.2 \pm 0.8$ and 3.6 ± 1.5 min, respectively).

Interestingly, the residence time of **1** was similar as **LEI101 (4)** ($RT = 14 \pm 6$ and 8.8 ± 1.6 min for **1** and **4**, respectively), despite a 10-fold lower binding affinity ($pK_i = 5.55 \pm 0.08$ and 6.51 ± 0.09 for **1** and **4**, respectively), which was due to the very low k_{on} value of **1** ($2.2 \pm 1.0 \times 10^3 \text{ M}^{-1}\text{s}^{-1}$).

5.2.5 Influence of physicochemical properties on affinity and binding kinetics

Next, the effects of physicochemical properties on equilibrium affinity and binding kinetics were analyzed. Hence, the cLogP (**Table 1**) of the compounds with varying alkyl R^2 substituents (group A) and the basicity (pK_a) with varying amine R^1 substituents (group B) were plotted against equilibrium affinity, association rate k_{on} and residence time. The basicity of group B did not correlate with any of the measured parameters (pK_i : Pearson r : 0.02328, p -value = 0.9064; k_{on} : Pearson r : -0.2213, p -value = 0.6735; RT : Pearson r : 0.3944, p -value = 0.5112). In case of group A, a near-significant correlation was identified with their lipophilicity and equilibrium affinity (Pearson r : 0.692, p -value = 0.0542, **Figure 4A**), but not with k_{on} (Pearson r : 0.1452, p -value = 0.7561, **Figure 4B**). Interestingly, cLogP of group A was highly correlated with residence time (Pearson r : 0.8869, p -value = 0.0078, **Figure 4C**). Noteworthy, this correlation was not observed with the R^1 substituents of group B (**Figure 5**).

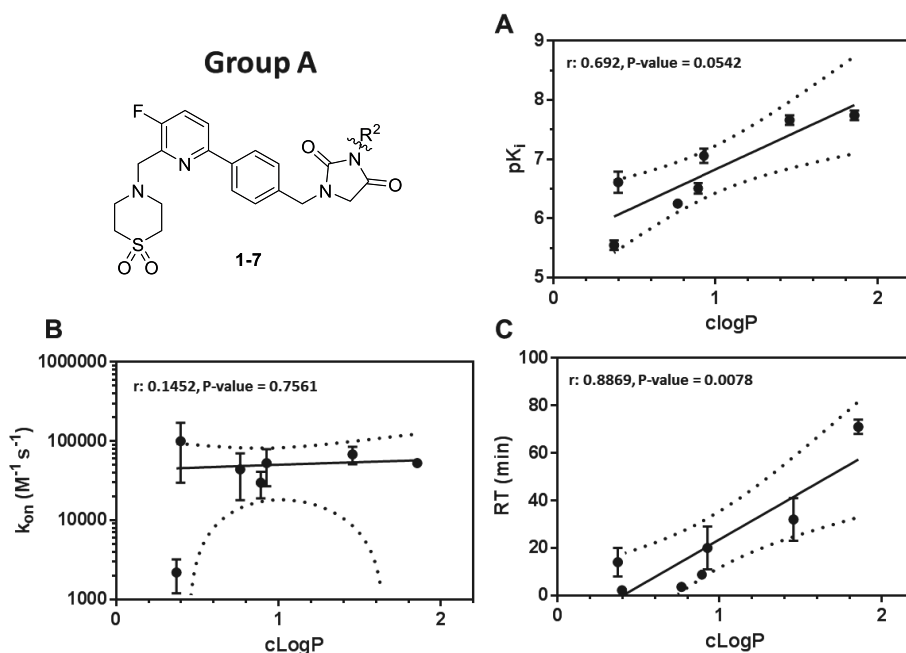


Figure 4. Correlation plots of lipophilicity and binding kinetics of group A agonists. A-C) Correlation plot of equilibrium affinity (A), association rate k_{on} (B) or residence time (RT) (C) with cLogP values. Correlation analysis was performed using a two-tailed Pearson correlation analysis (r = Pearson coefficient). All data shown with errors are the mean and SEM of three independent experiments performed in duplicate.

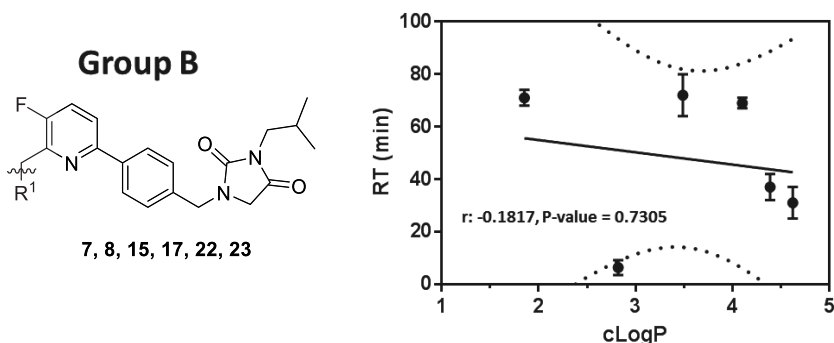


Figure 5. Correlation plots of lipophilicity and binding kinetics of group B agonists. Correlation plot of residence time (RT) and cLogP values. Correlation analysis was performed using a two-tailed Pearson correlation analysis (r = Pearson coefficient). Data shown with errors are the mean and SEM of three independent experiments performed in duplicate.

5.2.6 Influence of binding kinetics on functional activity

Finally, the influence of residence time on functional activity of the compound library was investigated. To this end, both groups were characterized in two functional assays: GTPγS binding and β -arrestin recruitment (**Table 2**). All compounds displayed partial agonism in both assays relative to CP55940. The highest intrinsic efficacy was observed for **5** in the G protein activation assay ($E_{\max} = 79 \pm 14\%$), whereas agonist **2** had the highest efficacy in the β -arrestin recruitment assay ($E_{\max} = 76 \pm 15\%$). The lowest efficacy was observed for **1** in both functional assays (β -arrestin: $E_{\max} = 25 \pm 2\%$; GTPγS: $E_{\max} = 48 \pm 7\%$). Generally, agonists showed a lower efficacy for β -arrestin recruitment, except for agonists **2**, **6** and **15** (E_{\max} β -arrestin: 76 ± 15 , 62 ± 8 and 64 ± 10 compared to E_{\max} GTPγS: 54 ± 13 , 50 ± 2 and 65 ± 12 , respectively), although these differences were not significant. Indeed, no correlation was observed between the efficacies of the compounds in the two functional assays (Pearson r : 0.04247, p -value = 0.1688). In addition, no correlation between residence time and *in vitro* efficacy was identified (GTPγS Pearson r : 0.00621, p -value: 0.9895; β -arrestin Pearson r : 0.1053, p -value 0.8222). For example, the long residence time of agonists **6**, **7**, **8**, **17**, **22** and **23** did not have a higher efficacy than the other agonists in either functional assay. In fact, agonist **2** with the shortest residence time (2.2 ± 0.8 min) had a very moderate efficacy in GTPγS ($54 \pm 13\%$), and the highest efficacy of all agonists for β -arrestin recruitment ($76 \pm 15\%$).

The potencies ranged from 6.06 ± 0.27 (**3**) to 7.94 ± 0.24 (**7**) in the GTPγS assay, whereas in the β -arrestin recruitment assay the potencies ranged from 6.12 ± 0.23 (**1**) to 8.14 ± 0.08 (**22**). In contrast to efficacy, the potency of the compounds was similar and highly correlated in the two functional assays (Pearson r : 0.8445, p -value < 0.0005). In general the compounds showed a higher potency in β -arrestin recruitment assays. For example, **22** showed a 17-fold higher potency for β -arrestin recruitment compared to G protein activation ($pEC_{50} = 8.14 \pm 0.08$ and 6.91 ± 0.32 , respectively).

Notably, nanomolar potency ($pEC_{50} > 7.5$) was only displayed by agonists with a residence time of at least 30 min as exemplified by compounds **6**, **8** and **23** (with residence times of 32 ± 9 , 37 ± 5 and 31 ± 6 min, respectively) and compounds **7**, **17** and **22** ($RT = 71 \pm 3$, 72 ± 8 and 69 ± 2 min, respectively). A statistically significant correlation was found for the residence times of group A with functional potency for both G protein activation and β -arrestin recruitment (**Figure 6A-B**). Interestingly, the residence times of group B did not correlate with either potency or efficacy (GTP γ S E_{max} Pearson r : 0.0021, p -value: 0.9968; pEC_{50} Pearson r : 0.3391, p -value: 0.5108; β -arrestin E_{max} Pearson r : -0.2591, p -value: 0.6200; pEC_{50} Pearson r : 0.6586, p -value: 0.1549).

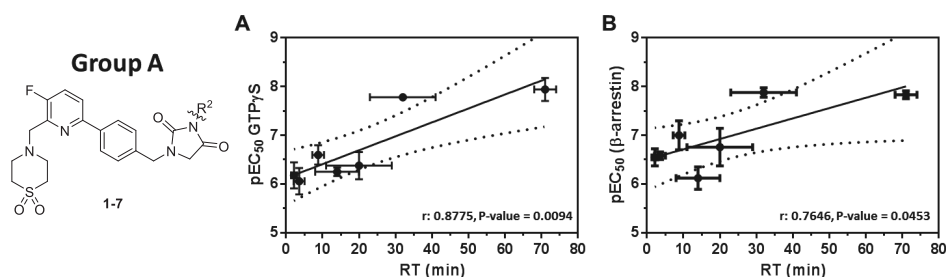


Figure 6. Correlation plots of residence time and potency of Group A agonists. Correlation plot of potency (pEC_{50}) in G protein activation (A) or β -Arrestin (B) with residence time (RT). Correlation analysis was performed using a two-tailed Pearson correlation analysis (r = Pearson coefficient). Data shown with errors are the mean and SEM of three independent experiments performed in duplicate.

5.3 Discussion

5.3.1 Kinetic characterization of LEI101-based agonists

Recently, drug discovery research has focused on the development of selective CB₂R agonists for the treatment of tissue injury and inflammatory diseases that avoid inducing CB₁R-mediated psychoactive side effects. CB₂R knockout mice show enhanced pathology in various inflammatory disease models, including heart, liver or kidney injury and inflammatory pain, thereby supporting the notion that CB₂R plays an essential role in these conditions. Despite compelling proof-of-concept data obtained in preclinical pain models, several CB₂R agonists lacked efficacy in phase 2 clinical trials for unknown reasons.^{30, 31}

Drug-target binding kinetics and their influence on functional activity are increasingly considered in drug discovery because it may aid in the design of lead compounds.³ Therefore, the relationships between functional activity and binding kinetics of a series of 24 agonists was investigated, based on the CB₂R-selective agonist **LEI101**, which showed *in vivo* efficacy in the treatment of neuropathic pain and inflammation-induced tissue damage.^{27, 28} The measured equilibrium binding affinities corresponded to previously determined structure-activity relationships (SAR) for this scaffold.²⁸

Using a high-throughput kinetic screening assay, based on its equivalent for the Adenosine A₁ receptor,²⁹ agonists with R¹ = dioxidethiomorpholine (group A) and R² = isobutyl (group B) were selected for full kinetic characterization (**Figure 2A**). It was found that the kinetic profile of the agonists had smaller variations in k_{on} values, but larger variations in k_{off} values, which were visualized using a kinetic map of the agonist library (**Figure 2C**). For this series of compounds, binding affinity was mostly influenced by their dissociation rate, as illustrated by a significant correlation with k_{off} values, but not with k_{on} values. (**Figure 3C,D**). This observation was similar as reported for the Muscarinic M₃ receptor and the adenosine A_{2A} receptor,^{17, 18} but in contrast to reports on β_2 adrenergic receptors and the hERG channel, for which the association rate was found to be the main driving force in ligand affinity.^{32, 33}

5.3.2 The role of physicochemical properties on binding kinetics and functional activity

Previously, it has been shown that controlling physicochemical properties such as lipophilicity and basicity can lead to 'tuned drug-target binding kinetics'.^{9, 34, 35} Therefore the library was divided into two groups in which either the lipophilicity or the basicity was systematically varied at different locations of the scaffold. This way, the relationships between physicochemical properties, binding kinetics and functional activity of these agonists could be investigated, for which two independent signaling pathways were used; G protein activation and β -arrestin recruitment. A significant correlation was found between increasing lipophilicity at the R² position of the LEI101 scaffold and residence time (group A agonists, **Figure 4C**), but not for the R¹ position (group B agonists, **Figure 5**). By dividing the compound library in two parts, it was shown that there is a lipophilic binding domain in the receptor targeted by the R² substituents. Occupying this pocket increases binding affinity due to decreased dissociation rate. Hence, it is not the overall lipophilicity of a molecule that determines its dissociation rate, but rather the lipophilicity at a specific position of the scaffold.³⁴ These findings fit well with the observation that any relationships between physicochemical properties and binding kinetics are both ligand and target specific and constitute the molecular underpinning of the lipophilic efficiency index.³⁶

Currently, there is no CB₂R crystal structure available to validate the positioning of this lipophilic binding domain, but a lipophilic binding domain was identified in the active site of CB₁R, formed by six amino acid residues,^{37, 38} of which four (i.e. Val114^{3,32}, Tyr191^{5,39}, Leu192^{5,40} and Met275^{6,55}) are conserved in the CB₂R active site.³⁹ This indicates that these residues may also play a role in the formation of a lipophilic binding domain responsible for the increased residence time of LEI101-based agonists with lipophilic R² substituents.

All compounds were identified as partial agonists in two signaling pathways, G protein activation and β -arrestin recruitment relative to CP55940 that behaved as a full agonist.⁴⁰ This indicates that these molecules, despite differences in binding kinetics, do not show any biased agonism. Interestingly, nanomolar potency for G protein activation and β -arrestin recruitment was associated with compounds having a residence time longer than 30 min, as a significant correlation between dissociation rate and functional potency for both assays was identified (**Figure 6**).

Again, this observation was specific for group A agonists. No correlation between residence time and functional efficacy was identified, as was reported for the Adenosine A₁ receptor.⁴¹ This observation is in contrast with the previously reported positive correlation found between residence time and efficacy, but not potency, for the Adenosine A_{2A} receptor and Muscarinic M3 receptor.^{17, 18} Of note, for both GPCRs these molecules showed significant longer residence times than the LEI101-based agonist library.

5.3.3 Target-specific binding kinetics in drug discovery

Interestingly, the kinetic profile of this agonist library shows remarkable differences compared to the reported binding kinetics of some structurally different synthetic ligands for CB₂R, like JWH133 and SR144528 and endocannabinoids anandamide (AEA) and noladin ether (NE), which all had divergent, but relatively fast kinetics.⁴² For these molecules, the association rate was the main driving force for their affinity. Knowledge of the kinetic binding parameters of a target's endogenous ligands is important for two reasons: 1) it is an indication of the ligand binding kinetics necessary to maintain homeostasis and 2) these play a major role in defining the pharmacological effect of a drug, as they have to compete with the endogenous ligands for binding to the active site.^{43, 44} Notably, LEI101, identified to be *in vivo* active in the treatment of neuropathic pain and inflammation-induced tissue damage,^{27, 28} has similar binding kinetics as 2-AG, relative to CP55940 (10-fold slower k_{on} , 10-fold faster k_{off}).⁴² This may indicate that slow association plays a role in the *in vivo* efficacy of LEI101. Interestingly, HU308 and JWH133, also *in vivo* active CB₂R-selective agonists (see **Chapter 4**),^{31, 45, 46} had slower association rates,⁴² but a similar dissociation rate, relative to CP55940 (20-50-fold slower k_{on} , similar k_{off}). This may indicate that the optimal kinetic profile of *in vivo* active CB₂R agonists is flexible, or may be dependent on disease type and/or progression. Although, it is noted that species differences between mouse and human CB₂R have not been taken into account.

Interestingly, slowly associating ligands may decrease on-target related side effects by preventing high target occupancy and fast target activation.¹⁵ This could be important, because prolonged activation of CB₂R is hypothesized to interfere with the ECS homeostasis.^{42, 47} Specifically, local, transient activation of CB₂R by endocannabinoids may lead to immunosuppression in the early phases of the immune response, perhaps via apoptotic mechanisms.^{48, 49} Rapid restoration of cellular activity might also be required to counteract potential infectious threats.⁵⁰ This indicates that the optimal kinetic profile of novel molecules needs to be established according to their functional activity, and should always be a combination of association and dissociation rates, resulting in an optimal level of receptor occupancy *in vivo*.⁵¹

5.4 Conclusions

To conclude, this chapter reports the structure-kinetics-relationship of LEI101-based agonists of the cannabinoid CB₂ receptor. The lipophilicity of the R² position was identified as important feature to increase receptor residence time, which correlated with increased potency, but not with efficacy, in two signaling pathways: G protein activation and β -arrestin recruitment. The findings of this study provide important insights into how CB₂R agonists can be designed with desired kinetic profiles for the future development of novel treatments of inflammatory diseases (**Chapter 1**).

5.5 Experimental Section

5.5.1 Chemistry

5.5.1.1 General remarks

All reagents and solvents were purchased from commercial sources and are of analytical grade. All reagents and solvents were used without any further purification. All steps were performed under an Argon atmosphere, unless stated otherwise. Organic solvents used were dried using molecular sieves prior to use for reactions, unless stated otherwise. Demineralized water is referred to as H₂O and is used in all cases, unless stated otherwise. Thin-layer Chromatography (TLC) was used to monitor the progress of the reactions, using aluminum coated Merck silica gel F254 plates. Solutions were concentrated using a Heidolph laborota W8 4000 efficient rotary evaporator with a Laboport vacuum pump. Purification by column chromatography was performed using Screening Devices B.V. silica gel (40–63 μ m). Purification by preparative thin layer chromatography was performed using Merck PCL Silica gel 60 F254 plates (1 mm). Purification by Preparative High-Performance Liquid Chromatography (Prep-HPLC) was performed using a Phenomenex Gemini C18 5 μ m 110Å 21.2 x 150 mm column, measuring UV absorbance at 254 nm using a Waters 2998 PDA UV detector and the m/z ratio using an Acquity Single Quad (Q1) detector. The sample was injected in the system in fractions of 100 – 500 μ l by a Waters 2767 Sample Manager and after running through the column in a gradient of ACN and Milli-Q water (+0.1% TFA), the fraction containing the reported mass was collected by the fraction collector of the Waters 2767 Sample Manager. ¹H and ¹³C NMR spectra were recorded on a Bruker AV 400 liquid, AV 400 imaging or a AV 600 spectrometer at ambient temperature, using CDCl₃, CD₃OD, DMSO-*d*₆, D₂O or CD₃CN as solvent. Chemical shift values are reported in ppm with TMS or solvent resonance as the internal standard (CDCl₃/TMS, δ 0.00 for ¹H (TMS), δ 77.16 for ¹³C (CDCl₃); CD₃OD, δ 3.31 for ¹H, δ 49.00 for ¹³C; CD₃CN, δ 1.94 for ¹H, δ 1.32 for ¹³C; DMSO, δ 2.50 for ¹H, δ 39.52 for ¹³C; D₂O, δ 4.79 for ¹H). Data are reported as follows: chemical shifts (δ) in ppm, multiplicity (s = singlet, br s = broad singlet, d = doublet, dd = doublet of doublet, t = triplet, q = quartet, m = multiplet), coupling constants *J* (Hz), and integration. Analytical purity was determined by Liquid Chromatography Mass Spectroscopy (LCMS) using a Phenomenex Gemini C18 5 μ m 110Å 4.6 x 150 mm analytical column, measuring UV absorbance at 254 nm by using a Waters 2998 PDA UV detector and the m/z ratio by using an Acquity Single Quad (Q1) detector. High resolution mass spectra were recorded by direct injection (2 μ L of a 2 μ M solution in water/acetonitrile 50/50 (v/v) and 0.1% formic acid) on a mass spectrometer (Thermo Finnigan LTQ Orbitrap) equipped with an electrospray ion source in positive mode (source voltage 3.5 kV, sheath gas flow 10, capillary temperature 250°C) with resolution *R* = 60,000 at m/z 400 (mass range m/z = 150–2,000) and dioctylphthalate (m/z = 391.28428) as a “lock mass”. The high resolution mass spectrometer was calibrated prior to measurements with a calibration mixture (Thermo Finnigan).

5.5.1.2 Synthetic procedures of intermediates 28a-g and agonists 1, 9 and 18 (Scheme 1)

(6-Bromo-3-fluoropyridin-2-yl)methanol (26): 6-Bromo-3-fluoropicolinaldehyde (**25**, 2.040 g, 10 mmol, 1 eq.) was dissolved in DCM:MeOH (2:1, 45 mL) and NaBH₄ (0.397 g, 10.50 mmol, 1.05 eq.) was added portionwise. The reaction mixture was stirred at rt for 80 min. Brine was added, and the layers were separated. The aqueous layer was extracted with DCM (3x) and the combined organic layers were dried with MgSO₄, filtered and concentrated *in vacuo*, to afford the title compound as a white powder (2.03 g, 9.9 mmol, 99%). ¹H NMR (400 MHz, CDCl₃) δ 7.42 (dd, *J* = 8.5, 3.5 Hz, 1H), 7.30 (t, *J* = 8.5 Hz, 1H), 4.81 (d, *J* = 1.9 Hz, 2H), 3.39 (br s, 1H).

(6-Bromo-3-fluoropyridin-2-yl)methyl methanesulfonate (27): (6-Bromo-3-fluoropyridin-2-yl)methanol (**26**, 3.25 g, 15.9 mmol, 1 eq.) was dissolved in THF (80 mL) and Et₃N (4.91 mL, 35.2 mmol, 2.2 eq.) was added. The reaction mixture was cooled to 0°C. MsCl (1.8 mL, 23.9 mmol, 1.5 eq.) was added dropwise and the reaction mixture was stirred for 45 min at 0°C. After completion of the reaction, the mixture was concentrated *in vacuo*. The residue was dissolved in DCM and water was added. The water layer was extracted 3 times with DCM. The combined organic layers were washed with brine, dried with MgSO₄, filtered and concentrated *in vacuo*, to yield the title compound as a yellow-ish solid (3.25 g, 11.5 mmol, 72%). ¹H NMR (400 MHz, CDCl₃): δ 7.54 (dd, *J* = 8.0, 3.6 Hz, 1H), 7.38 (t, *J* = 8.4 Hz, 1H), 5.36 (s, 2H), 3.16 (s, 3H).

General procedure to building blocks 28a-g

(6-Bromo-3-fluoropyridin-2-yl)methyl methanesulfonate **27** (1 eq.) was dissolved in ACN (0.2M). K₂CO₃ (2.2 eq.) and the corresponding secondary amine of the R₁ substituent (1.2 eq) were added. The reaction mixture was stirred at 50°C until TLC analysis showed complete conversion of the starting material. The reaction mixture was cooled to room temperature (rt) and water and DCM were added. The layers were separated and the waterlayer was extracted with DCM (3x). The combined organic layers were washed with brine, dried with MgSO₄, filtered and concentrated *in vacuo*.

4-((6-Bromo-3-fluoropyridin-2-yl)methyl)thiomorpholine 1,1-dioxide (28a): Prepared from thiomorpholine 1,1-dioxide (0.58 g, 4.26 mmol, 1.2 eq.) as the corresponding secondary amine of the R₁ substituent. The crude product was purified using silica gel column chromatography (5 to 40% EtOAc in PE), to yield the title compound as a white solid (0.56 g, 1.72 mmol, 49% yield). ¹H NMR (400 MHz, CDCl₃) δ 7.47 (dd, *J* = 3.6, 8.8 Hz, 1H), 7.35 (t, *J* = 4.6 Hz, 1H), 3.92 (s, 2H), 3.16 – 3.13 (m, 8H).

6-Bromo-2-((3,3-difluoropiperidin-1-yl)methyl)-3-fluoropyridine (28b): Prepared from 3,3-difluoropiperidine (0.43 g, 2.73 mmol, 1.2 eq.) as the corresponding secondary amine of the R₁ substituent. The product was obtained as a white to orange solid (0.63 g, 2.18 mmol, 95% yield). ¹H NMR (400 MHz, CDCl₃) δ 7.36 (dd, *J* = 8.8, 17.2 Hz, 1H), 7.29 (t, *J* = 4.4 Hz, 1H), 3.86 (d, *J* = 2.8 Hz, 2H), 2.79 (t, *J* = 11.6 Hz, 2H), 2.59 (t, *J* = 5.0 Hz, 2H), 1.89 – 1.75 (m, 4H).

4-((6-Bromo-3-fluoropyridin-2-yl)methyl)morpholine (28c): Prepared from morpholine (0.24 mL, 2.77 mmol, 1.2 eq.) as the corresponding secondary amine of the R₁ substituent. The product was obtained as a light yellow solid (0.44 g, 1.61 mmol, 71% yield). ¹H NMR (400 MHz, CDCl₃) δ 7.40 (dd, *J* = 5.2, 8.4 Hz, 1H), 7.27 (t, *J* = 6.2 Hz, 1H), 3.72 (br s, 6H), 2.58 (t, *J* = 4.6 Hz, 4H).

6-Bromo-2-((4,4-difluoropiperidin-1-yl)methyl)-3-fluoropyridine (28d): Prepared from 4,4-difluoropiperidine (0.46 g, 2.87 mmol, 1.2 eq.) as the corresponding secondary amine of the R₁ substituent. The product was obtained as a white to orange solid (0.66 g, 2.12 mmol, 92% yield). ¹H NMR (400 MHz, CDCl₃) δ 7.41 (dd, *J* = 3.6, 8.8 Hz, 1H), 7.30 (t, *J* = 4.6 Hz, 1H), 3.77 (d, *J* = 6.0 Hz, 2H), 2.68 (t, *J* = 5.6 Hz, 4H), 2.05 – 1.95 (m, 4H).

6-Bromo-3-fluoro-2-(piperidin-1-ylmethyl)pyridine (28e): Prepared from piperidine (0.20 mL, 2.75 mmol, 1.2 eq.) as the corresponding secondary amine of the R₁ substituent.

The product was obtained as a yellow to orange solid (0.56 g, 2.07 mmol, 90% yield). ^1H NMR (400 MHz, CDCl_3) δ 7.37 (dd, $J = 5.2, 8.8$ Hz, 1H), 7.26 (t, $J = 5.6$ Hz, 1H), 3.69 (d, $J = 2.4$ Hz, 2H), 2.51 (br s, 4H), 1.61 – 1.55 (m, 4H), 1.42 – 1.41 (m, 2H).

6-Bromo-3-fluoro-2-((4-methylpiperidin-1-yl)methyl)pyridine (28): Prepared from 4-methylpiperidine (0.33 mL, 2.73 mmol, 1.2 eq.) as the corresponding secondary amine of the R_1 substituent. The crude product was purified using silica gel column chromatography (5 to 20% EtOAc in PE). The product was obtained as a yellow solid (0.53 g, 1.86 mmol, 80% yield). ^1H NMR (400 MHz, CDCl_3) δ 7.38 (dd, $J = 3.6, 8.8$ Hz, 1H), 7.26 (t, $J = 8.4$ Hz, 1H), 3.69 (d, $J = 2.8$ Hz, 2H), 2.93 (d, $J = 11.6$ Hz, 2H), 2.10 (t, $J = 11.6$ Hz, 2H), 1.59 (d, $J = 11.6$ Hz, 2H), 1.33 – 1.23 (m, 3H), 0.90 (d, $J = 6.0$ Hz, 3H).

1-((6-Bromo-3-fluoropyridin-2-yl)methyl)-4-methylpiperazine (28g): Prepared from *N*-methylpiperazine (0.30 mL, 2.73 mmol, 1.2 eq.) as the corresponding secondary amine of the R_1 substituent. The product was obtained as an orange solid (0.45 g, 1.57 mmol, 69% yield). ^1H NMR (400 MHz, CDCl_3) δ 7.38 (dd, $J = 4.8, 8.4$ Hz, 1H), 7.27 (t, $J = 7.6$ Hz, 1H), 3.75 (d, $J = 2.4$ Hz, 2H), 2.62 (br s, 4H), 2.45 (br s, 4H), 2.28 (s, 3H).

General procedure to intermediates 29a,c,e

Building block **28a**, **28c** or **28e** (1 eq.) was dissolved in Toluene/EtOH (4:1, degassed). (4-Formylphenyl)boronic acid (1.5 eq.), $\text{Pd}(\text{PPh}_3)_4$ (0.05 eq.) and K_2CO_3 (4 eq.) were added. The reaction mixture was stirred overnight at 75°C . After completion of the reaction, the mixture was cooled to rt. Water and EtOAc were added and the layers were separated. The waterlayer was extracted three times with EtOAc. The combined organic layers were washed with water and brine, dried with Na_2SO_4 , filtered and concentrated *in vacuo*.

4-6-((1,1-Dioxidothiomorpholino)methyl)-5-fluoropyridin-2-yl)benzaldehyde (29a): Prepared from building block **28a** (0.05 g, 0.16 mmol, 1 eq.). The product was purified by silica gel column chromatography (0 to 40% MeOH in PE). The crude product was obtained as a yellow oil (53 mg, 0.15 mmol, quantitative yield). ^1H NMR (400 MHz, CDCl_3) δ 10.11 (s, 1H), 8.14 (d, $J = 7.6$ Hz, 2H), 8.01 (d, $J = 6.0$ Hz, 2H), 7.82 (t, $J = 6.6$ Hz, 1H), 7.72 – 7.67 (m, 1H), 4.07 (s, 2H), 3.25 (br s, 4H), 3.14 (br s, 4H).

4-(5-Fluoro-6-(morpholinomethyl)pyridin-2-yl)benzaldehyde (29c): Prepared from building block **28c** (0.05 g, 0.18 mmol, 1 eq.). The product was purified by silica gel column chromatography (0 to 40% MeOH in PE). The crude product was obtained as a yellow oil (54 mg, 0.18 mmol, quantitative yield). ^1H NMR (400 MHz, CDCl_3) δ 10.10 (s, 1H), 8.16 (d, $J = 8.0$ Hz, 2H), 8.03 – 8.99 (m, 2H), 7.82 (d, $J = 7.6$ Hz, 1H), 7.78 – 7.76 (m, 1H), 3.90 (s, 2H), 3.77 (br s, 4H), 2.71 (br s, 4H).

4-(5-Fluoro-6-(piperidin-1-ylmethyl)pyridin-2-yl)benzaldehyde (29e): Prepared from building block **28e** (0.05 g, 0.18 mmol, 1 eq.). The product was purified by silica gel column chromatography (0 to 40% MeOH in PE). The product was obtained as a yellow oil (35 mg, 0.11 mmol, 60%). ^1H NMR (400 MHz, CDCl_3) δ 10.07 (s, 1H), 8.14 (d, $J = 8.0$ Hz, 2H), 7.98 – 7.97 (m, 2H), 7.74 (d, $J = 5.2$ Hz, 1H), 7.48 (d, $J = 6.8$ Hz, 1H), 3.87 (s, 2H), 2.63 (br s, 4H), 1.64 (br s, 4H), 1.43 (br s, 2H).

General procedure for the synthesis of agonists 1, 9 and 18 (three steps)

Biaryl aldehyde **29a**, **29c** or **29e** (1 eq.) was dissolved in THF/MeOH (0.2 M, 3:1, dry) at a concentration of 0.2 M. Methyl glycinate (2 eq.) and Sodium triacetoxymethylborohydride (2 eq.) were added. The reaction mixture was stirred at rt until TLC analysis showed completion of the reaction, which was generally overnight. After completion of the reaction, water, Et_3N and EtOAc were added and the layers were separated. The waterlayer was extracted three times with EtOAc containing 1% Et_3N . The combined organic layers were washed with water and brine, dried with MgSO_4 , filtered and concentrated *in vacuo*. The crude product was obtained as a yellow solid and used in the next step without further purification.

The product mass was confirmed by TLC-MS. Biaryl methyl glycinate **30a**, **30c** or **30e** (1 eq.) was dissolved in DCM/water (1:1). Sodium cyanate (2 eq.) and acetic acid (2 eq.) were added. The mixture was stirred at rt until completion, generally less than 1 hr. After completion of the reaction the reaction mixture was concentrated *in vacuo* and coevaporated with toluene. The crude product was obtained as a yellow solid and used in the next step without further purification. The product mass was confirmed by TLC-MS. Biaryl urea acetamide **31a**, **31c** or **31e** (1 eq.) was dissolved in MeOH. Sodium methoxide (3 eq.) was added and the reaction mixture was stirred at rt until completion, which was generally overnight. After completion of the reaction, water and EtOAc were added. The waterlayer was extracted with EtOAc three times. The combined organic layers were washed with water and brine, dried with MgSO_4 , filtered and concentrated *in vacuo*.

1-(4-(6-((1,1-Dioxidothiomorpholino)methyl)-5-fluoropyridin-2-yl)benzyl)imidazolidine-2,4-dione (1):

Prepared in three steps from biaryl aldehyde **29a** (0.06 g, 0.22 mmol, 1 eq.). The product was purified by silica gel column chromatography (0 to 5% MeOH in DCM) and subsequently with preparative HPLC. The product was obtained as a colorless solid (14.07 mg, 0.033 mmol, 18% yield (over 3 steps)). ^1H NMR (600 MHz, CD_3CN) δ 8.52 (s, 1H), 8.05 (d, J = 8.4 Hz, 2H), 7.91 (dd, J = 3.6, 8.7 Hz, 1H), 7.66 (t, J = 9.0 Hz, 1H), 7.40 (d, J = 7.8 Hz, 2H), 4.52 (s, 2H), 4.34 (d, J = 1.8 Hz, 2H), 3.81 (s, 2H), 3.62 – 3.60 (m, 4H), 3.36 – 3.35 (m, 4H). ^{13}C NMR (150 MHz, CD_3CN) δ 171.8, 159.5, 157.8, 153.5, 153.4, 141.4, 141.3, 138.9, 138.0, 129.3, 128.2, 125.9, 125.7, 123.3, 123.2, 55.5, 52.0, 51.6, 50.1, 46.5. LCMS purity > 95%, (ESI) m/z calculated for $\text{C}_{20}\text{H}_{22}\text{FN}_4\text{O}_4\text{S}$ $[\text{M}+\text{H}]^+$: 433.1340, found: 433.1339.

1-(4-(5-Fluoro-6-(morpholinomethyl)pyridin-2-yl)benzyl)imidazolidine-2,4-dione (9):

Prepared in three steps from biaryl aldehyde **29c** (0.06 g, 0.21 mmol, 1 eq.). The product was purified by silica gel column chromatography (0 to 5% MeOH in DCM) and subsequently with preparative HPLC. The product was obtained as a colorless solid (31.35 mg, 0.082 mmol, 43% yield (over 3 steps)). ^1H NMR (600 MHz, CD_3CN) δ 8.73 (s, 1H), 8.06 (d, J = 7.8 Hz, 2H), 7.94 (dd, J = 3.6, 9.0 Hz, 1H), 7.69 (t, J = 9.0 Hz, 1H), 7.40 (d, J = 8.4 Hz, 2H), 4.51 (d, J = 2.0 Hz, 4H), 3.95 (br s, 4H), 3.80 (s, 2H), 3.59 (br s, 2H), 3.26 (br s, 2H). ^{13}C NMR (150 MHz, CD_3CN) δ 171.9, 159.5, 157.7, 153.8, 153.7, 139.0, 138.3, 138.2, 137.7, 129.3, 128.3, 126.2, 126.1, 123.8, 123.8, 64.5, 55.4, 53.3, 51.6, 47.3, 46.5, 31.4. LCMS purity > 95%, HRMS (ESI) m/z calculated for $\text{C}_{20}\text{H}_{22}\text{FN}_4\text{O}_3$ $[\text{M}+\text{H}]^+$: 385.1670, found: 385.1672.

1-(4-(5-Fluoro-6-(piperidin-1-ylmethyl)pyridin-2-yl)benzyl)imidazolidine-2,4-dione (18):

Prepared in three steps from biaryl aldehyde **29e** (0.06 g, 0.22 mmol, 1 eq.). The product was purified by silica gel column chromatography (0 to 5% MeOH in DCM) and subsequently with preparative HPLC. The product was obtained as a colorless solid (7.6 mg, 0.020 mmol, 9% yield (over 3 steps)). ^1H NMR (600 MHz, CD_3CN) δ 8.60 (br s, 1H), 8.07 (d, J = 8.4 Hz, 2H), 7.96 (dd, J = 3.6, 8.4 Hz, 1H), 7.69 (t, J = 9.0 Hz, 1H), 7.41 (d, J = 8.4 Hz, 2H), 4.53 (s, 2H), 4.45 (d, J = 1.8 Hz, 2H), 3.81 (s, 2H), 3.63 (d, J = 6.8 Hz, 2H), 3.11 – 3.09 (m, 2H), 3.04 (br s, 2H), 1.89 (t, J = 7.6 Hz, 4H). ^{13}C NMR (150 MHz, CD_3CN) δ 171.8, 159.4, 157.7, 153.7, 153.7, 139.1, 138.7, 137.7, 129.3, 128.3, 126.0, 123.7, 123.7, 55.2, 54.5, 51.6, 47.1, 46.5, 23.6, 22.2, 9.0. LCMS purity > 95%, HRMS (ESI) m/z calculated for $\text{C}_{21}\text{H}_{24}\text{FN}_4\text{O}_2$ $[\text{M}+\text{H}]^+$: 383.1878, found: 383.1879.

5.5.1.3 Synthetic procedures of intermediates 35a-g and agonists 2-8, 10-17 and 19-24 (Scheme 2)

2-((4-Bromobenzyl)amino)acetamide (33A): NaOH (4.40 g, 110 mmol, 1.1 eq.) was added to a mixture of 4-bromobenzaldehyde (**32**, 18.50 g, 100 mmol, 1 eq.) and 2-aminoacetamide-HCl (12.16 g, 110 mmol, 1.1 eq.) in methanol/water (5:1, 520 mL). The reaction was stirred for 20 hr at rt. Then the reaction mixture was cooled to 0°C and NaBH_4 (3.78 g, 100 mmol, 1 eq.) was added portionwise. The mixture was stirred for an additional 6 hr, then the mixture was acidified until pH=3. The mixture was subsequently neutralized with concentrated NaHCO_3 and the methanol was removed under reduced pressure. The white creamy substance was filtered off and dried under vacuum, yielding a white powder (19.29 g, 79 mmol, 79%). ^1H NMR (400 MHz, MeOD) δ 7.63 (d, J = 8.4 Hz, 2H), 7.46 (d, J = 8.4 Hz, 2H), 4.24 (s, 2H), 3.84 (s, 2H).

1-(4-Bromobenzyl)imidazolidine-2,4-dione (34A): 2-((4-Bromobenzyl)amino)acetamide (**33A**, 7.29 g, 30 mmol, 1 eq.) was dissolved in acetonitrile (125 mL) and CDI (9.73, 60 mmol, 2 eq.) and DMAP (7.33 g, 60 mmol, 2 eq.) were added. After stirring 48 hr at 60°C, the reaction mixture was cooled to rt, and quenched with 1 M aqueous HCl. The aqueous phase was extracted with EtOAc (3x) and the combined organic layers were washed with water, brine and dried with MgSO₄, filtered and concentrated under reduced pressure. The crude product was purified using silica gel column chromatography (40-60% EtOAc in PE). The product was obtained as a yellow solid (3.901 g, 14.5 mmol, 48% yield). ¹H NMR (400 MHz, CDCl₃) δ 7.51 (d, *J* = 8.4 Hz, 2H), 7.15 (d, *J* = 8 Hz, 2H), 4.49 (s, 2H), 3.80 (s, 2H).

General procedure for the synthesis of building blocks 35a-b and 35d-g

1-(4-bromobenzyl)imidazolidine-2,4-dione **34A** (1 eq.) was dissolved in DMF (0.2M). K₂CO₃ (3 eq.) and the corresponding alkylhalide for the R² substituent (2 eq.) were added. The reaction mixture was stirred at 50°C until TLC analysis showed complete conversion of the starting material. The reaction mixture was cooled to rt and water and Et₂O were added. The layers were separated and the waterlayer was extracted three times with Et₂O. The combined organic layers were washed with brine, dried with MgSO₄, filtered and concentrated *in vacuo*.

1-(4-Bromobenzyl)-3-methylimidazolidine-2,4-dione (35a): Prepared from iodomethane (0.9 mL, 11.2 mmol, 2 eq.) as the corresponding alkylhalide of the R² substituent. The product was obtained as an orange to red oil (1.63 g, 5.6 mmol, quantitative yield). ¹H NMR (400 MHz, CDCl₃) δ 7.48 (d, *J* = 8.0 Hz, 2H), 7.15 (d, *J* = 8.4 Hz, 2H), 4.52 (s, 2H), 3.74 (s, 2H), 3.04 (s, 3H).

1-(4-Bromobenzyl)-3-(2-methoxyethyl)imidazolidine-2,4-dione (35b): Prepared from 2-bromo ethylmethyl ether (0.71 mL, 7.6 mmol, 2 eq.) as the corresponding alkylhalide of the R² substituent. The product was obtained as a yellow oil (1.20 g, 3.7 mmol, 98% yield). ¹H NMR (400 MHz, CDCl₃) δ 7.49 (d, *J* = 11.6 Hz, 2H), 7.14 (d, *J* = 8.0 Hz, 2H), 4.52 (s, 2H), 3.76 – 3.73 (m, 4H), 3.60 (t, *J* = 5.4 Hz, 2H), 3.34 (d, *J* = 11.2 Hz, 3H).

1-(4-Bromobenzyl)-3-ethylimidazolidine-2,4-dione (35d): Prepared from bromoethane (0.8 mL, 11.2 mmol, 2 eq.) as the corresponding alkylhalide of the R² substituent. The product was obtained as an orange to red oil (1.26 g, 4.25 mmol, 77% yield). ¹H NMR (400 MHz, CDCl₃) δ 7.49 (d, *J* = 8.4 Hz, 2H), 7.14 (d, *J* = 8.4 Hz, 2H), 4.51 (s, 2H), 3.71 (s, 2H), 3.59 (q, *J* = 7.2 Hz, 2H), 1.26 – 1.22 (m, 3H).

1-(4-Bromobenzyl)-3-propylimidazolidine-2,4-dione (35e): Prepared from 1-bromopropane (1.02 mL, 11.2 mmol, 2 eq.) as the corresponding alkylhalide of the R² substituent. The product was obtained as an orange to red oil (1.55 g, 5.0 mmol, 90% yield). ¹H NMR (400 MHz, CDCl₃) δ 7.49 (d, *J* = 8.0 Hz, 2H), 7.13 (d, *J* = 8.0 Hz, 2H), 4.52 (s, 2H), 3.72 (s, 2H), 3.50 (t, *J* = 6.8 Hz, 2H), 1.66 (q, *J* = 7.2 Hz, 2H), 0.93 (t, *J* = 7.4 Hz, 3H).

1-(4-Bromobenzyl)-3-isobutylimidazolidine-2,4-dione (35f): Prepared from 1-bromo-2-methylpropane (1.2 mL, 11.2 mmol, 2 eq.) as the corresponding alkylhalide of the R² substituent. The product was obtained as an orange/red oil (1.39 g, 4.3 mmol, 77% yield). ¹H NMR (400 MHz, CDCl₃) δ 7.49 (d, *J* = 8.0 Hz, 2H), 7.14 (d, *J* = 7.6 Hz, 2H), 4.52 (s, 2H), 3.73 (s, 2H), 3.35 (d, *J* = 7.2 Hz, 2H), 2.10 – 2.05 (m, 1H), 0.92 (d, *J* = 6.8 Hz, 6H).

1-(4-Bromobenzyl)-3-butyylimidazolidine-2,4-dione (35g): Prepared from 1-bromobutane (1.2 mL, 11.2 mmol, 2 eq.) as the corresponding alkylhalide of the R₂ substituent. The product was obtained as an orange/red oil (1.68 g, 5.2 mmol, 94% yield). ¹H NMR (400 MHz, CDCl₃) δ 7.49 (dd, *J* = 2.0, 6.8 Hz, 2H), 7.13 (d, *J* = 8.4 Hz, 2H), 4.51 (s, 2H), 3.72 (s, 2H), 3.52 (t, *J* = 7.4 Hz, 2H), 1.65 – 1.58 (m, 2H), 1.37 – 1.32 (m, 2H), 0.94 (t, *J* = 7.2 Hz, 3H).

(4-Bromobenzyl)glycine (33B): Glycine (9.25 g, 83 mmol, 1.05 eq.) was dissolved in water (40 mL). 4-bromobenzaldehyde (**32**, 14.61 g, 79 mmol, 1 eq.) was dissolved in MeOH (220 mL) and added to the glycine solution. A solution of NaOH (2 M, 31.6 mL, 63.2 mmol, 0.8 eq.) was added. The reaction mixture was stirred for 10 min at rt and subsequently cooled to 0°C. NaBH₄ (2.99 g, 79 mmol, 1 eq.) was added portionwise. The reaction mixture was stirred for 40 hr at rt. The MeOH was removed under reduced pressure and the aqueous layer was washed twice with Et₂O. The aqueous layer then was acidified with 1 M HCl until pH = 1 and the precipitate was collected by filtration and washed with Et₂O. The solid was coevaporated twice with acetone. The white creamy substance was dried under vacuum, yielding the product as a white powder (17.36 g, 71.1 mmol, 90% yield). ¹H NMR (400 MHz, DMSO-*d*₆) δ 7.62 (d, *J* = 8.4 Hz, 2H), 7.52 (d, *J* = 8.4 Hz, 2H), 4.13 (s, 2H), 3.80 (s, 2H).

2-((4-Bromobenzyl)amino)-*N*-cyclopropylacetamide (34B): (4-Bromobenzyl)glycine (**33B**, 10.67 g, 27.3 mmol, 1 eq.) was dissolved in water (110 mL). Triethylamine (11.3 mL, 82 mmol, 3 eq.) was added. After all solid was dissolved, Boc anhydride (6.3 mL, 27.3 mmol, 1 eq.) was added. The mixture was stirred overnight at rt. A 10% KHSO₄ solution was added and the mixture was extracted twice with EtOAc and once with DCM. The combined organic layers were dried with MgSO₄, filtered and concentrated *in vacuo*. The residue (7.81 g, 22.7 mmol, 1 eq.) was dissolved in dry DCM (160 mL). DMF (0.5 mL) and thionyl chloride (2.7 mL, 81.7 mmol, 3.6 eq.) were added and the reaction mixture was stirred for 3.5 hr at rt. After completion, the reaction mixture was concentrated *in vacuo*. The intermediate was dissolved in dry DCM (300 mL) and was cooled down to 0°C. Cyclopropylamine (2.6 mL, 36.3 mmol, 1.6 eq.) was added dropwise. The mixture was stirred overnight at 0°C. DCM and water were added. The layers were separated and the water layer was extracted with DCM (3x). The combined organic layers were washed with brine, dried with MgSO₄, filtered and concentrated *in vacuo* and under high vacuum. Product was obtained as a dark yellow solid (6.21 g, 22.0 mmol, 81% over three steps). ¹H NMR (400 MHz, CDCl₃) δ 7.42 (d, *J* = 8.0 Hz, 2H), 7.16 (d, *J* = 8.4 Hz, 2H), 3.68 (s, 2H), 3.19 (s, 2H), 2.70 – 2.64 (m, 1H), 0.75 – 0.71 (m, 2H), 0.48 – 0.44 (m, 2H).

1-(4-Bromobenzyl)-3-cyclopropylimidazolidine-2,4-dione (35c): 2-((4-bromobenzyl)amino)-*N*-cyclopropyl acetamide (**34B**, 2.83 g, 10 mmol, 1 eq.) was dissolved in ACN (50 mL) and DMAP (3.25 g, 26.6 mmol, 2.66 eq.) and CDI (3.24 g, 20 mmol, 2 eq.) were added. The reaction mixture was stirred overnight at 60°C. After completion, the reaction mixture was cooled down to rt and sat. aq. NaHCO₃ was added. The layers were separated and the aqueous layer was extracted with EtOAc (3x). The combined organic layers were washed with brine, dried with MgSO₄, filtered and concentrated *in vacuo*. Crude product was purified using silica gel column chromatography (30 to 50% EtOAc in PE). The title compound was obtained as a yellow solid (2.91 g, 9.40 mmol, 94% yield). ¹H NMR (400 MHz, CDCl₃) δ 7.49 (d, *J* = 8 Hz, 2H), 7.13 (d, *J* = 8.4 Hz, 2H), 4.49 (s, 2H), 3.66 (s, 2H), 2.62 (t, *J* = 5.6 Hz, 1H), 0.97 (d, *J* = 5.6 Hz, 4H)

General procedure for the synthesis of agonists 2-8, 10-17 and 19-24

Building block **35a**, **35b**, **35c**, **35d**, **35e**, **35f** or **35g** was dissolved in DMF (degassed, 0.2 M). KOAc (4.4 eq.), bis(pinacolato)diboron (1.5 eq.) and Pd(dppf)Cl₂ (0.056 eq.) were added. The reaction mixture was stirred overnight at 75°C. After completion of the reaction, the mixture was cooled to rt. Water and EtOAc were added and the layers were separated. The waterlayer was extracted three times with EtOAc. The combined organic layers were washed with sat. aq. NaHCO₃, water and brine, dried with MgSO₄, filtered and concentrated *in vacuo*. The residue was coevaporated with CHCl₃ three times. The pinacol esters were all yielded as a brown oil and used in the next step without any further purification due to instability of the pinacol ester. Next, pinacol ester **36a**, **36b**, **36c**, **36d**, **36e**, **36f** or **36g** (1.5 eq.) was dissolved in degassed toluene/ethanol (4:1) at a concentration of 0.2M. Bromide building block **28a**, **28b**, **28c**, **28d**, **28e**, **28f** or **28g** (1 eq.), Pd(PPh₃)₄ (0.1 eq.) and K₂CO₃ (6 eq.) were added. The reaction mixture was stirred at 75°C until completion, which was generally overnight. After completion of the reaction, the mixture was cooled to rt and filtered. Water and EtOAc were added and the layers were separated.

The waterlayer was extracted three times with EtOAc. The combined organic layers were washed with water and brine, dried with MgSO₄, filtered and concentrated *in vacuo*.

1-(4-(6-((1,1-Dioxidothiomorpholino)methyl)-5-fluoropyridin-2-yl)benzyl)-3-methylimidazolidine-2,4-dione (2): Prepared from building block **28a** (0.044 g, 0.14 mmol, 1 eq.) and pinacol ester **36a** (0.067 g, 0.21 mmol, 1.5 eq.). Purification by silica gel column chromatography (0 - 1% MeOH in DCM) and subsequently with preparative HPLC yielded the product as a white solid (48.09 mg, 0.108 mmol, 53%). ¹H NMR (600 MHz, CD₃CN) δ 8.06 (d, *J* = 7.8 Hz, 2H), 7.90 (dd, *J* = 3.6, 8.4 Hz, 1H), 7.64 (t, *J* = 9.0 Hz, 1H), 7.39 (d, *J* = 8.4 Hz, 2H), 4.57 (s, 2H), 4.32 (d, *J* = 1.8 Hz, 2H), 3.77 (s, 2H), 3.59 (t, *J* = 4.2 Hz, 4H), 3.34 (d, *J* = 4.8 Hz, 4H), 2.93 (s, 3H). ¹³C NMR (150 MHz, CD₃CN) δ 171.4, 159.5, 158.3, 157.8, 153.4, 153.4, 141.6, 141.5, 138.8, 138.0, 129.3, 128.2, 125.8, 125.7, 123.1, 123.1, 55.5, 51.9, 50.5, 50.2, 46.8, 25.1. LCMS purity > 95%, HRMS (ESI) *m/z* calculated for C₂₁H₂₄FN₄O₄S [M+H]⁺: 447.1497, found: 447.1495.

1-(4-(6-((1,1-Dioxidothiomorpholino)methyl)-5-fluoropyridin-2-yl)benzyl)-3-(2-methoxyethyl)imidazolidine-2,4-dione (3): Prepared from building block **28a** (0.036 g, 0.11 mmol, 1 eq.) and pinacol ester **36b** (0.061 g, 0.16 mmol, 1.5 eq.). The product was purified by silica gel column chromatography (0 - 4% MeOH in DCM) and subsequently with preparative HPLC. The product was obtained as a yellow oil (49.71 mg, 0.101 mmol, 62%). ¹H NMR (600 MHz, CD₃CN) δ 8.05 (d, *J* = 8.4 Hz, 2H), 7.94 (dd, *J* = 3.6, 8.4 Hz, 1H), 7.69 (t, *J* = 6.0 Hz, 1H), 7.40 (d, *J* = 7.8 Hz, 2H), 4.58 (s, 2H), 4.49 (d, *J* = 1.8 Hz, 2H), 3.81 (s, 2H), 3.78 - 3.76 (m, 4H), 3.64 (t, *J* = 5.7 Hz, 2H), 3.54 (t, *J* = 5.7 Hz, 2H), 3.45 (d, *J* = 3.2 Hz, 4H), 3.30 (s, 3H), 2.65 (s, 3H). ¹³C NMR (150 MHz, CD₃CN) δ 171.3, 159.3, 158.1, 157.6, 153.7, 139.9, 139.8, 138.9, 137.8, 129.4, 128.3, 126.2, 126.1, 123.6, 69.7, 58.7, 55.2, 52.4, 50.4, 49.5, 46.8, 39.1. LCMS purity > 95%, HRMS (ESI) *m/z* calculated for C₂₃H₂₈FN₄O₅S [M+H]⁺: 491.1759, found: 491.1757.

3-Cyclopropyl-1-(4-(6-((1,1-dioxidothiomorpholino)methyl)-5-fluoropyridin-2-yl)benzyl)imidazolidine-2,4-dione (4, LEI101): Prepared from building block **28a** (0.036 g, 0.11 mmol, 1 eq.) and pinacol ester **36c** (0.060 g, 0.17 mmol, 1.5 eq.). The product was purified by silica gel column chromatography (0 - 4% MeOH in DCM) and subsequently with preparative HPLC. The product was obtained as a white oil (39.55 mg, 0.084 mmol, 53%). ¹H NMR (600 MHz, CD₃CN) δ 8.04 (d, *J* = 8.4 Hz, 2H), 7.93 (dd, *J* = 3.6, 9.0 Hz, 1H), 7.67 (t, *J* = 9.0 Hz, 1H), 7.38 (d, *J* = 7.8 Hz, 2H), 4.53 (s, 2H), 4.46 (d, *J* = 1.8 Hz, 2H), 3.76 (t, *J* = 5.4 Hz, 4H), 3.68 (s, 2H), 3.46 (s, 4H), 2.54 - 2.51 (m, 1H), 0.88 - 0.85 (m, 4H). ¹³C NMR (150 MHz, CD₃CN) δ 171.8, 159.4, 148.4, 157.7, 153.6, 153.6, 140.0, 139.9, 138.9, 137.8, 129.3, 128.2, 126.1, 125.9, 123.5, 123.5, 68.9, 55.1, 52.2, 50.0, 49.6, 46.8, 22.2, 5.3, 31.4. LCMS purity > 95%, HRMS (ESI) *m/z* calculated for C₂₃H₂₆FN₄O₄S [M+H]⁺: 473.1653, found: 473.1651.

1-(4-(6-((1,1-Dioxidothiomorpholino)methyl)-5-fluoropyridin-2-yl)benzyl)-3-ethylimidazolidine-2,4-dione (5): Prepared from building block **28a** (0.038 g, 0.12 mmol, 1 eq.) and pinacol ester **36d** (0.062 g, 0.18 mmol, 1.5 eq.). The product was purified by silica gel column chromatography (0 - 2% MeOH in DCM) and subsequently with preparative HPLC. The product was obtained as a yellowish oil (52.92 mg, 0.115 mmol, 63%). ¹H NMR (600 MHz, CD₃CN) δ 8.04 (d, *J* = 8.4 Hz, 2H), 7.92 (dd, *J* = 3.6, 8.4 Hz, 1H), 7.69 (t, *J* = 3.0 Hz, 1H), 7.40 (d, *J* = 7.8 Hz, 2H), 4.57 (s, 2H), 4.44 (d, *J* = 1.8 Hz, 2H), 3.78 (s, 2H), 3.71 (t, *J* = 3.2 Hz, 4H), 3.50 (q, *J* = 4.8 Hz, 2H), 3.41 (t, *J* = 4.8 Hz, 4H), 1.16 (t, *J* = 7.2 Hz, 3H). ¹³C NMR (150 MHz, CD₃CN) δ 171.3, 159.3, 158.1, 157.6, 153.6, 140.4, 140.3, 138.9, 137.9, 129.4, 128.3, 126.1, 126.0, 123.5, 55.3, 52.3, 50.5, 49.7, 46.8, 34.6, 13.7. LCMS purity > 95%, HRMS (ESI) *m/z* calculated for C₂₂H₂₆FN₄O₄S [M+H]⁺: 461.1653, found: 461.1651.

1-(4-(6-((1,1-Dioxidothiomorpholino)methyl)-5-fluoropyridin-2-yl)benzyl)-3-propylimidazolidine-2,4-dione (6): Prepared from building block **28a** (0.036 g, 0.11 mmol, 1 eq.) and pinacol ester **36e** (0.060 g, 0.17 mmol, 1.5 eq.). The product was purified by silica gel column chromatography (0 - 2% MeOH in DCM) and subsequently with preparative HPLC. The product was obtained as an off-white oil (30.19 mg, 0.064 mmol, 38%).

¹H NMR (600 MHz, CD₃CN) δ 8.03 (d, *J* = 8.4 Hz, 2H), 7.89 (dd, *J* = 3.6, 8.4 Hz, 1H), 7.64 (t, *J* = 9.0 Hz, 1H), 7.39 (d, *J* = 9.6 Hz, 2H), 4.57 (s, 2H), 4.29 (d, *J* = 1.8 Hz, 2H), 3.78 (s, 2H), 3.55 – 3.53 (m, 4H), 3.42 (t, *J* = 7.2 Hz, 2H), 3.30 (t, *J* = 3.4 Hz, 4H), 1.61 (q, *J* = 4.8 Hz, 2H), 0.90 (t, *J* = 7.2 Hz, 3H). ¹³C NMR (150 MHz, CD₃CN) δ 171.3, 158.5, 158.2, 157.8, 153.4, 153.3, 142.0, 141.9, 138.8, 138.1, 129.2, 128.2, 125.8, 125.6, 123.0, 123.0, 55.7, 51.9, 50.3, 46.8, 41.1, 22.2, 11.5. LCMS purity > 95%, HRMS (ESI) *m/z* calculated for C₂₃H₂₈FN₄O₄S [M+H]⁺: 475.1810, found: 475.1808.

1-(4-(6-((1,1-Dioxidothiomorpholino)methyl)-5-fluoropyridin-2-yl)benzyl)-3-isobutylimidazolidine-2,4-dione (7):

Prepared from building block **28a** (0.039 g, 0.12 mmol, 1 eq.) and pinacol ester **36f** (0.067 g, 0.18 mmol, 1.5 eq.). The product was purified by silica gel column chromatography (0 - 6% MeOH in DCM) and subsequently with preparative HPLC. The product was obtained as a yellow oil (38.11 mg, 0.078 mmol, 43%). ¹H NMR (400 MHz, CD₃CN) δ 8.05 (d, *J* = 8.4 Hz, 2H), 7.93 (dd, *J* = 3.6, 8.8 Hz, 1H), 7.67 (t, *J* = 9.0 Hz, 1H), 7.39 (d, *J* = 8.4 Hz, 2H), 4.57 (s, 2H), 4.48 (d, *J* = 2.0 Hz, 2H), 3.80 – 3.77 (m, 6H), 3.48 (d, *J* = 4.4 Hz, 4H), 3.26 (d, *J* = 7.2 Hz, 2H), 2.05 – 1.97 (m, 1H), 0.88 (d, *J* = 9.6 Hz, 6H). ¹³C NMR (100 MHz, CD₃CN) δ 171.5, 159.8, 158.4, 157.2, 153.6, 153.6, 139.8, 139.6, 139.0, 137.7, 129.2, 128.2, 126.1, 125.9, 123.6, 123.5, 118.4, 55.0, 52.2, 50.3, 49.4, 46.8, 46.8, 31.4, 28.3, 20.3. LCMS purity > 95%, HRMS (ESI) *m/z* calculated for C₂₄H₃₀FN₄O₄S [M+H]⁺: 489.1966, found: 489.1964.

1-(4-(6-((3,3-Difluoropiperidin-1-yl)methyl)-5-fluoropyridin-2-yl)benzyl)-3-isobutylimidazolidine-2,4-dione (8):

Prepared from building block **28b** (0.037 g, 0.12 mmol, 1 eq.) and pinacol ester **36f** (0.067 g, 0.18 mmol, 1.5 eq.). The product was purified by silica gel column chromatography (0 - 6% MeOH in DCM) and subsequently with preparative HPLC. The product was obtained as a yellow oil (24.79 mg, 0.052 mmol, 61%). ¹H NMR (600 MHz, CD₃CN) δ 8.08 (d, *J* = 8.4 Hz, 2H), 7.98 (dd, *J* = 3.6, 8.4 Hz, 1H), 7.71 (t, *J* = 9.0 Hz, 1H), 7.42 (d, *J* = 8.4 Hz, 2H), 4.59 (s, 2H), 4.55 (d, *J* = 1.2 Hz, 2H), 3.83 (s, 2H), 3.61 (t, *J* = 11.1 Hz, 2H), 3.40 (s, 2H), 3.29 (d, *J* = 7.2 Hz, 2H), 2.16 – 2.12 (m, 2H), 2.11 – 2.05 (m, 2H), 2.04 – 2.01 (m, 1H), 0.92 (d, *J* = 6.6 Hz, 6H). ¹³C NMR (150 MHz, CD₃CN) δ 171.5, 159.5, 158.5, 158.4, 157.8, 153.7, 153.6, 139.1, 138.8, 138.7, 137.8, 139.1, 138.8, 138.7, 137.8, 129.3, 128.2, 126.2, 126.1, 123.7, 123.6, 121.8, 120.2, 55.7, 55.5, 55.3, 55.2, 52.6, 50.4, 46.9, 46.8, 31.5, 31.1, 31.0, 30.8, 28.4, 20.3, 20.1, 20.1, 20.0. LCMS purity > 95%, HRMS (ESI) *m/z* calculated for C₂₅H₃₀F₃N₄O₂ [M+H]⁺: 475.2315, found: 475.2313.

1-(4-(5-Fluoro-6-(morpholinomethyl)pyridin-2-yl)benzyl)-3-methylimidazolidine-2,4-dione (10): Prepared from building block **28c** (0.037 g, 0.14 mmol, 1 eq.) and pinacol ester **36a** (0.067 g, 0.21 mmol, 1.5 eq.). The product was purified by silica gel column chromatography (0 - 5% MeOH in DCM) and subsequently with preparative HPLC. The product was obtained as a light brown solid (70.04 mg, 0.176 mmol, 87%). ¹H NMR (600 MHz, CD₃CN) δ 8.05 (d, *J* = 7.8 Hz, 2H), 7.95 (dd, *J* = 3.6, 5.4 Hz, 1H), 7.70 (t, *J* = 9.0 Hz, 1H), 7.40 (d, *J* = 7.8 Hz, 2H), 4.57 (s, 2H), 4.53 (s, 2H), 3.95 (br s, 4H), 3.79 (s, 2H), 3.53 – 3.34 (m, 4H), 2.93 (s, 3H). ¹³C NMR (150 MHz, CD₃CN) δ 171.6, 159.4, 157.7, 153.8, 153.8, 139.0, 138.2, 138.1, 137.7, 129.0, 128.3, 126.3, 126.1, 123.9, 123.9, 64.5, 55.4, 53.3, 50.6, 46.9, 25.2. LCMS purity > 95%, HRMS (ESI) *m/z* calculated for C₂₁H₂₄FN₄O₃ [M+H]⁺: 399.1827, found: 399.1824.

1-(4-(5-Fluoro-6-(morpholinomethyl)pyridin-2-yl)benzyl)-3-(2-methoxyethyl)imidazolidine-2,4-dione (11):

Prepared from building block **28c** (0.030 g, 0.11 mmol, 1 eq.) and pinacol ester **36b** (0.061 g, 0.16 mmol, 1.5 eq.). The product was purified by silica gel column chromatography (0 - 4% MeOH in DCM) and subsequently with preparative HPLC. The product was obtained as a yellow oil (47.33 mg, 0.107 mmol, 66%). ¹H NMR (600 MHz, CD₃CN) δ 8.07 (d, *J* = 8.4 Hz, 2H), 7.98 (dd, *J* = 3.6, 9.0 Hz, 1H), 7.72 (t, *J* = 9.0 Hz, 1H), 7.41 (d, *J* = 8.4 Hz, 2H), 4.59 (s, 2H), 4.54 (s, 2H), 3.96 (br s, 4H), 3.82 (s, 2H), 3.64 (t, *J* = 5.7 Hz, 2H), 3.54 (t, *J* = 5.7 Hz, 2H), 3.30 (s, 4H), 2.63 (s, 3H).

^{13}C NMR (150 MHz, CD_3CN) δ 171.4, 159.3, 158.1, 157.5, 153.8, 139.0, 137.7, 129.4, 128.3, 126.3, 126.2, 123.9, 69.7, 64.5, 58.7, 55.5, 53.5, 50.4, 46.9, 39.1. LCMS purity > 95%, HRMS (ESI) m/z calculated for $\text{C}_{23}\text{H}_{28}\text{FN}_4\text{O}_4$ $[\text{M}+\text{H}]^+$: 443.2089, found: 443.2087.

3-Cyclopropyl-1-(4-(5-fluoro-6-(morpholinomethyl)pyridin-2-yl)benzyl)imidazolidine-2,4-dione (12):

Prepared from building block **28c** (0.031 g, 0.11 mmol, 1 eq.) and pinacol ester **36c** (0.060 g, 0.17 mmol, 1.5 eq.). The product was purified by silica gel column chromatography (0 - 6% MeOH in DCM) and subsequently with preparative HPLC. The product was obtained as a white solid (35.75 mg, 0.084 mmol, 53%). ^1H NMR (400 MHz, CD_3CN) δ 8.06 (d, J = 8.4 Hz, 2H), 7.94 (dd, J = 3.6, 8.8 Hz, 1H), 7.68 (t, J = 8.8 Hz, 1H), 7.37 (d, J = 8 Hz, 2H), 4.53 (s, 2H), 4.48 (d, J = 1.6 Hz, 2H), 3.93 (br s, 4H), 3.68 (s, 2H), 3.55 (br s, 4H), 2.54 – 2.49 (m, 1H), 0.86 – 0.84 (m, 4H). ^{13}C NMR (100 MHz, CD_3CN) δ 171.7, 160.0, 158.3, 157.4, 153.7, 153.6, 139.0, 138.4, 138.3, 137.7, 129.3, 128.2, 126.1, 125.9, 123.8, 123.7, 118.4, 64.5, 55.3, 53.0, 50.0, 46.8, 22.1, 5.4, 31.4. LCMS purity > 95%, HRMS (ESI) m/z calculated for $\text{C}_{23}\text{H}_{26}\text{FN}_4\text{O}_3$ $[\text{M}+\text{H}]^+$: 425.1983, found: 425.1982.

3-Ethyl-1-(4-(5-fluoro-6-(morpholinomethyl)pyridin-2-yl)benzyl)imidazolidine-2,4-dione (13):

Prepared from building block **28c** (0.033 g, 0.12 mmol, 1 eq.) and pinacol ester **36d** (0.062 g, 0.18 mmol, 1.5 eq.). The product was purified by silica gel column chromatography (0 - 1% MeOH in DCM) and subsequently with preparative HPLC. The product was obtained as a white oil (25.62 mg, 0.062 mmol, 34%). ^1H NMR (400 MHz, CD_3CN) δ 8.06 (d, J = 8.4 Hz, 2H), 7.96 (dd, J = 3.6, 8.8, 1H), 7.70 (t, J = 9.2 Hz, 1H), 7.40 (d, J = 8.4 Hz, 2H), 4.56 (s, 2H), 4.51 (d, J = 1.6 Hz, 2H), 3.96 (br s, 4H), 3.77 (s, 2H), 3.58 (br s, 2H), 3.48 (q, J = 7.2 Hz, 2H), 3.25 (br s, 2H), 1.17 (t, J = 3.6 Hz, 3H). ^{13}C NMR (100 MHz, CD_3CN) δ 171.1, 159.8, 158.0, 157.2, 153.6, 139.1, 138.2, 138.1, 137.6, 129.2, 128.2, 126.2, 126.0, 123.8, 123.8, 118.4, 64.4, 55.3, 53.2, 34.4, 31.4, 13.7. LCMS purity > 95%, HRMS (ESI) m/z calculated for $\text{C}_{22}\text{H}_{26}\text{FN}_4\text{O}_3$ $[\text{M}+\text{H}]^+$: 413.1983, found: 413.1981.

1-(4-(5-Fluoro-6-(morpholinomethyl)pyridin-2-yl)benzyl)-3-propylimidazolidine-2,4-dione (14):

Prepared from building block **28c** (0.031 g, 0.11 mmol, 1 eq.) and pinacol ester **36e** (0.060 g, 0.17 mmol, 1.5 eq.). The product was purified by silica gel column chromatography (0 - 2% MeOH in DCM) and subsequently with preparative HPLC. The product was obtained as a colourless solid (21.35 mg, 0.050 mmol, 30%). ^1H NMR (600 MHz, CD_3CN) δ 8.07 (d, J = 7.8 Hz, 2H), 7.96 (dd, J = 3.6, 5.4 Hz, 1H), 7.69 (t, J = 8.4 Hz, 1H), 7.40 (d, J = 7.8 Hz, 2H), 4.57 (s, 2H), 4.51 (s, 2H), 3.95 (br s, 4H), 3.78 (s, 2H), 3.55 (br s, 2H), 3.42 (t, J = 4.6 Hz, 2H), 3.30 (br s, 2H), 1.64 – 1.58 (m, 2H), 0.90 (t, J = 7.5 Hz, 3H). ^{13}C NMR (150 MHz, CD_3CN) δ 171.4, 159.5, 158.3, 157.8, 153.8, 139.1, 138.3, 138.2, 137.7, 129.3, 128.3, 126.2, 126.1, 123.9, 123.8, 64.5, 55.4, 53.3, 50.5, 46.8, 41.2, 31.5, 22.2, 11.6. LCMS purity > 95%, HRMS (ESI) m/z calculated for $\text{C}_{23}\text{H}_{28}\text{FN}_4\text{O}_3$ $[\text{M}+\text{H}]^+$: 427.2140, found: 427.2137.

1-(4-(5-Fluoro-6-(morpholinomethyl)pyridin-2-yl)benzyl)-3-isobutylimidazolidine-2,4-dione (15):

Prepared from building block **28c** (0.030 g, 0.11 mmol, 1 eq.) and pinacol ester **36f** (0.062 g, 0.16 mmol, 1.5 eq.). The product was purified by silica gel column chromatography (0 - 6% MeOH in DCM) and subsequently with preparative HPLC. The product was obtained as a colorless solid (34.82 mg, 0.079 mmol, 49%). ^1H NMR (600 MHz, CD_3CN) δ 8.08 (d, J = 8.4 Hz, 2H), 7.98 (dd, J = 3.6, 9.0 Hz, 1H), 7.73 (t, J = 9.0 Hz, 1H), 7.42 (d, J = 8.4 Hz, 2H), 4.59 (s, 2H), 4.56 (d, J = 1.8 Hz, 2H), 4.01 (br s, 2H), 3.94 (br s, 2H), 3.83 (s, 2H), 3.62 (br s, 2H), 3.29 (d, J = 7.2 Hz, 4H), 2.05 – 2.01 (m, 1H), 0.92 (d, J = 7.2 Hz, 6H). ^{13}C NMR (150 MHz, CD_3CN) δ 171.5, 159.3, 158.4, 157.6, 153.8, 153.8, 139.2, 138.1, 138.0, 138.1, 138.0, 137.6, 129.3, 128.3, 126.3, 126.2, 123.9, 123.9, 64.4, 55.5, 55.5, 53.5, 50.4, 46.9, 46.8, 31.4, 28.4, 20.34. LCMS purity > 95%, HRMS (ESI) m/z calculated for $\text{C}_{24}\text{H}_{30}\text{FN}_4\text{O}_3$ $[\text{M}+\text{H}]^+$: 441.2296, found: 441.2295.

3-Butyl-1-(4-(5-fluoro-6-(morpholinomethyl)pyridin-2-yl)benzyl)imidazolidine-2,4-dione (16):

Prepared from building block **28c** (0.030 g, 0.11 mmol, 1 eq.) and pinacol ester **36g** (0.062 g, 0.17 mmol, 1.5 eq.).

The product was purified by silica gel column chromatography (0 - 4% MeOH in DCM) and subsequently with preparative HPLC. The product was obtained as a white solid (53.88 mg, 0.122 mmol, 73%). ¹H NMR (600 MHz, CD₃CN) δ 8.06 (d, *J* = 8.4 Hz, 2H), 7.95 (dd, *J* = 3.6, 8.4 Hz, 1H), 7.69 (t, *J* = 3.0 Hz, 1H), 7.39 (d, *J* = 7.8 Hz, 2H), 4.57 (s, 2H), 4.51 (d, *J* = 1.2 Hz, 2H), 3.95 (br s, 4H), 3.78 (s, 2H), 3.57 (br s, 2H), 3.45 (t, *J* = 7.2 Hz, 2H), 3.26 (br s, 2H), 1.58 – 1.56 (m, 2H), 1.33 (q, *J* = 5.2 Hz, 2H), 0.93 (t, *J* = 7.5 Hz, 3H). ¹³C NMR (150 MHz, CD₃CN) δ 171.3, 159.4, 158.2, 157.7, 153.7, 153.0, 139.0, 138.2, 138.1, 137.6, 129.2, 128.2, 126.2, 126.0, 123.8, 123.8, 64.4, 55.3, 53.2, 50.4, 46.4, 40.0, 39.3, 30.9, 20.6, 14.0. LCMS purity > 95%, HRMS (ESI) *m/z* calculated for C₂₄H₃₀FN₄O₃ [M+H]⁺: 441.2296, found: 441.2295.

1-(4-(6-((4,4-Difluoropiperidin-1-yl)methyl)-5-fluoropyridin-2-yl)benzyl)-3-isobutylimidazolidine-2,4-dione (17): Prepared from building block **28d** (0.033 g, 0.11 mmol, 1 eq.) and pinacol ester **36f** (0.062 g, 0.16 mmol, 1.5 eq.). The product was purified by silica gel column chromatography (0 - 6% MeOH in DCM) and subsequently with preparative HPLC. The product was converted to the HCl-salt by dissolving in EtOAc (5 mL) and adding HCl in dioxane (2 M, 0.085 mL). The precipitate was filtered off, subsequently purified with preparative HPLC and was obtained as a colourless solid (2.23 mg, 0.004 mmol, 2.5%). ¹H NMR (600 MHz, D₂O) δ 8.00 – 7.99 (m, 3H), 7.80 (t, *J* = 8.7 Hz, 1H), 7.47 (d, *J* = 8.4 Hz, 2H), 4.71 (s, 2H), 4.67 (s, 2H), 4.06 (s, 2H), 3.77 (br s, 4H), 3.33 (d, *J* = 7.8 Hz, 2H), 2.48 (br s, 4H), 1.99 (t, *J* = 6.9 Hz, 1H), 0.90 (d, *J* = 6.6 Hz, 6H). ¹³C NMR (150 MHz, D₂O) δ 173.3, 158.1, 158.0, 156.2, 152.9, 152.8, 136.6, 136.6, 136.2, 136.0, 118.5, 116.9, 128.0, 127.0, 125.4, 125.3, 123.6, 123.6, 53.3, 49.6, 49.5, 49.5, 49.2, 45.9, 45.5, 30.2, 30.1, 29.9, 26.6, 18.7. LCMS purity > 95%, HRMS (ESI) *m/z* calculated for C₂₅H₃₀F₃N₄O₂ [M+H]⁺: 475.2315, found: 475.2313.

1-(4-(5-Fluoro-6-(piperidin-1-ylmethyl)pyridin-2-yl)benzyl)-3-methylimidazolidine-2,4-dione (19): Prepared from building block **28e** (0.037 g, 0.14 mmol, 1 eq.) and pinacol ester **36a** (0.067 g, 0.21 mmol, 1.5 eq.). The product was purified by silica gel column chromatography (0 - 10% MeOH in DCM) and subsequently with preparative HPLC. The product was obtained as an off-white oil (44.01 mg, 0.111 mmol, 55%). ¹H NMR (600 MHz, CD₃CN) δ 8.06 (d, *J* = 8.4 Hz, 2H), 7.94 (dd, *J* = 3.6, 8.4 Hz, 1H), 7.67 (t, *J* = 9.0 Hz, 1H), 7.40 (d, *J* = 8.4 Hz, 2H), 4.57 (s, 2H), 4.44 (s, 2H), 3.78 (s, 2H), 3.63 (d, *J* = 6.4 Hz, 2H), 3.01 (br s, 2H), 2.93 (s, 3H), 1.87 (br s, 4H), 1.76 (br s, 1H), 1.46 (br s, 1H). ¹³C NMR (150 MHz, CD₃CN) δ 171.3, 159.5, 158.3, 157.7, 153.7, 153.6, 139.0, 138.8, 138.7, 137.8, 129.3, 128.2, 126.0, 125.9, 123.6, 123.6, 55.1, 54.2, 50.5, 46.8, 25.1, 23.5, 22.3. LCMS purity > 95%, HRMS (ESI) *m/z* calculated for C₂₂H₂₆FN₄O₂ [M+H]⁺: 397.2034, found: 397.2030.

1-(4-(5-Fluoro-6-(piperidin-1-ylmethyl)pyridin-2-yl)benzyl)-3-(2-methoxyethyl)imidazolidine-2,4-dione (20): Prepared from building block **28e** (0.030 g, 0.11 mmol, 1 eq.) and pinacol ester **36b** (0.061 g, 0.16 mmol, 1.5 eq.). The product was purified by silica gel column chromatography (0 - 6% MeOH in DCM) and subsequently with preparative HPLC. The product was obtained as a yellow oil (36.16 mg, 0.082 mmol, 50%). ¹H NMR (600 MHz, CD₃CN) δ 8.07 (d, *J* = 8.4 Hz, 2H), 7.97 (dd, *J* = 3.6, 9.0 Hz, 1H), 7.72 (t, *J* = 9.0 Hz, 1H), 7.42 (d, *J* = 7.8 Hz, 2H), 4.59 (s, 2H), 4.49 (d, *J* = 1.2 Hz, 2H), 3.82 (s, 2H), 3.65 – 3.60 (m, 4H), 3.54 (t, *J* = 5.7 Hz, 2H), 3.30 (s, 3H), 3.10 (t, *J* = 10.8 Hz, 2H), 2.63 (s, 4H), 1.90 – 1.85 (m, 2H), 1.83 – 1.80 (m, 1H), 1.53 – 1.51 (m, 1H). ¹³C NMR (150 MHz, CD₃CN) δ 171.4, 159.1, 158.1, 157.4, 153.7, 153.7, 139.0, 138.3, 138.2, 137.7, 129.4, 128.3, 126.3, 126.2, 123.8, 123.8, 69.7, 58.7, 55.2, 54.9, 50.5, 46.9, 39.1, 23.5, 22.1. LCMS purity > 95%, HRMS (ESI) *m/z* calculated for C₂₄H₃₀FN₄O₃ [M+H]⁺: 441.2296, found: 441.2294.

1-(4-(5-Fluoro-6-(piperidin-1-ylmethyl)pyridin-2-yl)benzyl)-3-propylimidazolidine-2,4-dione (21): Prepared from building block **28e** (0.031 g, 0.11 mmol, 1 eq.) and pinacol ester **36e** (0.060 g, 0.17 mmol, 1.5 eq.). The product was purified by silica gel column chromatography (0 - 2% MeOH in DCM) and subsequently with preparative HPLC. The product was obtained as a yellowish oil (25.62 mg, 0.062 mmol, 37%). ¹H NMR (600 MHz, CD₃CN) δ 8.07 (d, *J* = 7.8 Hz, 2H), 7.95 (dd, *J* = 3.6, 9.0 Hz, 1H), 7.69 (t, *J* = 9.0 Hz, 1H), 7.40 (d, *J* = 7.8 Hz, 2H), 4.57 (s, 2H), 4.45 (d, *J* = 1.2 Hz, 2H), 3.79 (s, 2H), 3.63 (d, *J* = 6.4 Hz, 2H), 3.42 (t, *J* = 7.2 Hz, 2H), 3.03 (br s, 2H), 1.89 (t, *J* = 3.6 Hz, 4H), 1.77 (br s, 1H), 1.64 – 1.58 (m, 2H), 1.47 (br s, 1H), 0.90 (t, *J* = 7.0 Hz, 3H).

^{13}C NMR (150 MHz, CD_3CN) δ 171.3, 159.4, 158.3, 157.7, 153.7, 153.7, 139.1, 137.7, 129.3, 128.2, 126.1, 126.0, 123.7, 123.6, 55.1, 54.4, 50.4, 46.8, 41.2, 23.5, 22.2, 22.2, 11.5. LCMS purity > 95%, HRMS (ESI) m/z calculated for $\text{C}_{24}\text{H}_{30}\text{FN}_4\text{O}_2$ $[\text{M}+\text{H}]^+$: 425.2347, found: 425.2343.

1-(4-(5-Fluoro-6-(piperidin-1-ylmethyl)pyridin-2-yl)benzyl)-3-isobutylimidazolidine-2,4-dione (22): Prepared from building block **28e** (0.033 g, 0.12 mmol, 1 eq.) and pinacol ester **36f** (0.067 g, 0.18 mmol, 1.5 eq.). The product was purified by silica gel column chromatography (0 - 8% MeOH in DCM) and subsequently with preparative HPLC. The product was obtained as a yellow oil (23.54 mg, 0.054 mmol, 30%). ^1H NMR (600 MHz, CD_3CN) δ 8.09 (d, J = 8.4 Hz, 2H), 7.98 (dd, J = 4.2, 9 Hz, 1H), 7.72 (t, J = 9 Hz, 1H), 7.43 (d, J = 8.4 Hz, 2H), 4.60 (s, 2H), 4.48 (s, 2H), 3.83 (s, 2H), 3.64 (d, J = 12 Hz, 2H), 3.29 (d, J = 7.2 Hz, 2H), 3.08 (br s, 2H), 2.05 – 2.01 (m, 1H), 1.93 – 1.89 (m, 4H), 1.82 – 1.80 (m, 1H), 1.53 – 1.50 (m, 1H), 0.92 (d, J = 6.6 Hz, 6H). ^{13}C NMR (600 MHz, CD_3CN) δ 171.5, 159.3, 158.4, 157.6, 153.7, 153.7, 139.2, 138.6, 138.5, 137.7, 129.3, 128.3, 126.2, 126.0, 123.7, 123.7, 55.2, 54.6, 50.4, 46.9, 31.5, 23.5, 22.2, 28.4, 20.3. LCMS purity > 95%, HRMS (ESI) m/z calculated for $\text{C}_{25}\text{H}_{32}\text{FN}_4\text{O}_2$ $[\text{M}+\text{H}]^+$: 439.2504, found: 439.2502.

1-(4-(5-Fluoro-6-((4-methylpiperidin-1-yl)methyl)pyridin-2-yl)benzyl)-3-isobutylimidazolidine-2,4-dione (23): Prepared from building block **28f** (0.034 g, 0.12 mmol, 1 eq.) and pinacol ester **36f** (0.067 g, 0.18 mmol, 1.5 eq.). The product was purified by silica gel column chromatography (0 - 6% MeOH in DCM) and subsequently with preparative HPLC. The product was obtained as a white solid (35.10 mg, 0.77 mmol, 50%). ^1H NMR (600 MHz, CD_3CN) δ 8.06 (d, J = 7.8 Hz, 2H), 7.95 (dd, J = 3.6, 8.4 Hz, 1H), 7.70 (t, J = 9 Hz, 1H), 7.41 (d, J = 8.4 Hz, 2H), 4.57 (s, 2H), 4.46 (s, 2H), 3.81 (s, 2H), 3.65 (d, J = 8.0 Hz, 2H), 3.27 (d, J = 7.8 Hz, 2H), 3.10 – 3.06 (m, 2H), 2.09 (s, 1H), 2.03 – 1.98 (m, 1H), 1.89 – 1.87 (m, 2H), 1.70 – 1.67 (m, 1H), 1.61 – 1.55 (m, 1H), 0.97 (d, J = 6.6 Hz, 3H), 0.90 (d, J = 7.2 Hz, 6H). ^{13}C NMR (150 MHz, CD_3CN) δ 170.1, 157.7, 157.0, 156.0, 152.2, 152.2, 137.7, 137.0, 136.9, 136.2, 127.8, 126.9, 126.8, 124.7, 124.6, 122.2, 122.2, 54.1, 53.3, 48.9, 45.4, 45.4, 30.5, 30.0, 27.8, 26.9, 19.8, 18.9. LCMS purity > 95%, HRMS (ESI) m/z calculated for $\text{C}_{26}\text{H}_{34}\text{FN}_4\text{O}_2$ $[\text{M}+\text{H}]^+$: 453.2660, found: 453.2655.

1-(4-(5-Fluoro-6-((4-methylpiperazin-1-yl)methyl)pyridin-2-yl)benzyl)-3-isobutylimidazolidine-2,4-dione (24): Prepared from building block **28g** (0.031 g, 0.11 mmol, 1 eq.) and pinacol ester **36f** (0.062 g, 0.16 mmol, 1.5 eq.). The product was purified by silica gel column chromatography (0 - 8% MeOH in DCM) and subsequently with preparative HPLC. The product was obtained as a white solid (44.76 mg, 0.099 mmol, 61%). ^1H NMR (400 MHz, CD_3CN) δ 8.05 (d, J = 8.4 Hz, 2H), 7.96 (dd, J = 3.6, 8.8 Hz, 1H), 7.69 (t, J = 9.0 Hz, 1H), 7.38 (d, J = 8.4 Hz, 2H), 4.57 (s, 2H), 4.52 (d, J = 1.6 Hz, 2H), 3.80 (s, 2H), 3.75 (br s, 4H), 3.60 (br s, 4H), 3.26 (d, J = 7.2 Hz, 2H), 2.85 (s, 3H), 2.05 – 1.97 (m, 1H), 0.90 (d, J = 6.4 Hz, 6H). ^{13}C NMR (100 MHz, CD_3CN) δ 171.5, 159.8, 158.4, 157.3, 153.8, 153.7, 139.1, 138.6, 138.4, 137.6, 129.2, 128.3, 126.2, 126.0, 123.9, 123.8, 118.9, 118.4, 55.0, 51.0, 50.3, 50.0, 46.9, 46.8, 43.5, 31.4, 28.4, 20.3. LCMS purity > 95%, HRMS (ESI) m/z calculated for $\text{C}_{25}\text{H}_{33}\text{FN}_5\text{O}_2$ $[\text{M}+\text{H}]^+$: 454.2613, found: 454.2611.

5.5.2 Biology

5.5.2.1 General remarks

$[\text{^3H}]\text{CP55940}$ (specific activity 141.2 Ci/mmol), $[\text{^35S}]\text{GTP}\gamma\text{S}$ (specific activity 1250 Ci/mmol) and GF-B/GF-C filters were purchased from Perkin Elmer (Waltham, MA). Bicinchoninic acid (BCA) and BCA protein assay reagent were obtained from Pierce Chemical Company (Rochford, IL). The PathHunter® CHO-K1 CNR1 (CHOK1hCB₁_bgal) and CNR2 (CHOK1hCB₂_bgal) β -Arrestin Cell Lines and the PathHunter® detection kit were obtained from DiscoverX. Cell culture plates were purchased from Sarstedt and 384-well white walled assay plates from Perkin Elmer. Cannabinoid receptor ligands CP55940 and AM630 were obtained from Sigma Aldrich (St. Louis, MO). All buffers and solutions were prepared using Millipore water (deionized using a MilliQ A10 Biocel™, with a 0.22 μm filter) and analytical grade reagents and solvents. Buffers are prepared at room temperature and stored at 4°C, unless stated otherwise.

5.5.2.2 Cell culture

CHOK1hCB₂_bgal cells were cultured in Ham's F12 Nutrient Mixture, supplemented with 10% fetal calf serum, 1 mM glutamine, 50 U/mL penicillin, 50 µg/mL streptomycin, 300 mg/mL hygromycin and 800 µg/mL geneticin in a humidified atmosphere at 37°C and 5% CO₂, as reported previously.³¹ Cells were subcultured twice a week at a ratio of 1:20 on 10-cm diameter plates by trypsinization. For membrane preparation the cells were subcultured 1:10 and transferred to 15-cm diameter plates. Cells were passaged no longer than 25 times or 3 months.

5.5.2.3 Membrane preparation

Per batch of membranes, cells on thirty 15-cm ø plates were detached from the bottom by scraping them into 5 mL phosphate-buffered saline (PBS), collected in 12 mL Falcon tubes and centrifuged for 5 min at 200 *g* (3,000 rpm). The pellets were resuspended in ice-cold 50 mM Tris-HCl buffer and 5 mM MgCl₂ (pH 7.4). An Ultra Thurrax homogenizer (Heidolph Instruments, Schwabach, Germany) was used to homogenize the cell suspension. The membranes and cytosolic fractions were separated by centrifugation at 100,000 *g* (31,000 rpm) in a Beckman Optima LE-80 K ultracentrifuge (Beckman Coulter Inc., Fullerton, CA) at 4°C for 20 min. The pellet was resuspended in 10 mL of Tris-HCl buffer and 5 mM MgCl₂ (pH 7.4) and the homogenization and centrifugation steps were repeated. Finally, the membrane pellet was resuspended in 10 mL 50 mM Tris-HCl buffer and 5 mM MgCl₂ (pH 7.4) and aliquots of 250 µL were stored at -80°C. Membrane protein concentrations were measured using the BCA method.⁵²

5.5.2.4 [³H]CP55940 equilibrium displacement assay

[³H]CP55940 displacement assays were used for the determination of affinity (IC₅₀) values of unlabeled ligands. Membrane aliquots containing 1.5 µg of membrane protein were incubated in a total volume of 100 µL assay buffer (50 mM Tris-HCl buffer (pH 7.4), 5 mM MgCl₂ and 0.1% BSA) at 25°C for 2 hr in presence of ~1.5 nM [³H]CP55940. Ten different concentrations of competing ligand were used for determination of IC₅₀ values, and nonspecific binding was determined in the presence of 10 µM AM630. Incubations were terminated and samples harvested as described by the 96-wells harvest procedure (see below).

5.5.2.5 96-wells harvest procedure

Samples were harvested on 96-wells GF/C filters, precoated with 25 µL 0.25% (v/v) PEI per well, with rapid vacuum filtration, to separate the bound and free radioligand, using a Perkin Elmer 96-wells harvester (Perkin Elmer, Groningen, The Netherlands). Filters were subsequently washed ten times with ice-cold assay buffer on the 96-well plate and 5 times on a wash plate. Filter plates were dried at 55°C for ~45 min, then 25 µL Microscint was added per well (Perkin Elmer, Groningen, The Netherlands). After 3 hr, the filter-bound radioactivity was determined by scintillation spectrometry using a Microbeta2® 2450 microplate counter (Perkin Elmer, Boston, MA).

5.5.2.6 [³H]CP55940 Association Assay

To determine association kinetics of [³H]CP55940, it was incubated at a concentration of ~1.5 nM with 1.5 µg of membrane protein in a total volume of 100 µL of assay buffer at 25°C or 10°C for a range of timepoints (90, 60, 30, 25, 20, 15, 10, 5, 3 and 1 min). For the assay at 10°C, an additional time point at 120 min was added. Nonspecific binding was determined in the presence of 10 µM AM630. Incubations were terminated and samples harvested as described by the 96-wells harvest procedure (see above).

5.5.2.7 [³H]CP55940 Dissociation Assay

To determine dissociation kinetics of [³H]CP55940, it was incubated at a concentration of ~1.5 nM with 1.5 µg of membrane protein in a total volume of 100 µL of assay buffer at 25°C or 10°C for 2 hr. Dissociation was then initiated at a range of timepoints (25°C: 90, 30, 20, 15, 10, 8, 5, 3, 1 min; 10°C: 360, 300, 240, 180, 120, 90, 60, 30, 10 and 5 min) by addition of 5 µL of AM630 (final assay concentration: 10 µM).

Nonspecific binding was determined by addition of 10 μM AM630 from the start of the assay. Incubations were terminated and samples harvested as described by the 96-wells harvest procedure (see above).

5.5.2.8 [^3H]CP55940 Dual-point Competition Association Assay

For fast determination of the relative kinetics of the agonist library, the KRI was determined using a dual-point competition association assay.¹³ The agonists were incubated at their IC_{50} concentration (as determined at 25°C) with 1.5 nM of [^3H]CP55940 and 1.5 μg membrane protein in assay buffer in a total volume of 100 μL , for either 1 or 2 hr at 10°C (t_1 and t_2 , respectively). Nonspecific binding was determined by addition of 10 μM AM630 from the start of the assay. Incubations were terminated and samples harvested as described by the 96-wells harvest procedure (see above).

5.5.2.9 [^3H]CP55940 Full Competition Association Assay

To determine the k_{on} and k_{off} values of unlabeled competing ligands. Ligands were incubated at their IC_{50} concentration (see 5.5.2.12 Data Analysis) in presence of ~ 1.5 nM [^3H]CP55940 and with 1.5 μg of membrane protein in a total volume of 100 μL of assay buffer at 10°C for a range of timepoints (120, 90, 60, 30, 25, 20, 15, 10, 5, 3 and 1 min). Nonspecific binding was determined in the presence of 10 μM AM630. Incubations were terminated and samples harvested as described by the 96-wells harvest procedure (see above).

5.5.2.10 [^{35}S]GTP γS assay

G protein activation as a measure for receptor activity was determined by the binding of radiolabeled non-hydrolyzable GTP ([^{35}S]GTP γS) to the receptor.^{31, 53} To homogenized CHOK1CB $_2$ R $_b$ gal membranes (5 μg) in 20 μL assay buffer (50 mM Tris-HCl buffer (pH 7.4), 5 mM MgCl_2 , 150 mM NaCl, 1 mM EDTA, 0.05% BSA and 1 mM DTT, freshly prepared every day), 5 μg saponin and 1 μM GDP were added (final assay concentration). To determine the pEC_{50} and E_{max} values of the agonist library, the membranes were directly incubated for 30 min at room temperature with various concentrations of the ligands of interest. The basal level of [^{35}S]GTP γS binding was measured in untreated membrane samples, and the maximal level of [^{35}S]GTP γS binding was measured by treatment of the membranes with 10 μM CP55940. Subsequently, [^{35}S]GTP γS (0.3 nM) was added and the samples were incubated for 90 min at 25 °C on a shaking platform in a total sample volume of 100 μL . Incubations were terminated and samples harvested as described by the 96-wells harvest procedure (see above). Here, samples were harvested on 96-wells GF/B filters and washed using buffer containing 50 mM Tris HCl, pH 7.4 and 5 mM MgCl_2 .

5.5.2.11 PathHunter® β -Arrestin Recruitment Assay

The assay was performed using the PathHunter® CHOK1CB $_2$ R $_b$ gal cells and β -arrestin recruitment assay kit (DiscoverX Corporation, Fremont, CA), as published before.^{31, 54} Briefly, PathHunter® CHOK1hCB $_2$ R $_b$ gal cells were seeded at a density of 5000 cells per well of solid white walled 384-well plates (Perkin Elmer, MA, USA) in 20 μL HAM's F12 Nutrient Mixture culture medium and incubated overnight in a humidified atmosphere at 37°C and 5% CO_2 . The cells were stimulated with 5 μL of 50 μM (10 μM final assay concentration) of each agonist (single point assay) or 10 increasing concentrations of each agonist and incubated for 90 min in a humidified atmosphere at 37°C and 5% CO_2 . The DMSO concentration was the same in each well (0.25%). The activity of β -galactosidase was determined using the PathHunter® Detection Kit (DiscoverX Corporation, Fremont, CA), following the supplier's protocol. In short, the cells were loaded with 12 μL detection reagent (DiscoverX Corporation, Fremont, CA) and incubated for 1 hr in the dark at room temperature. Luminescence (400-700 nm), indicated as relative light units (RLU), was measured on an EnVision multilabel plate reader (Perkin Elmer, MA, USA), using a Luminescence 700 emission filter.

5.5.2.12 Data Analysis

cLogP and pK_a values were calculated using ChemDraw® Professional 16.0 (Perkin Elmer). All experimental data were analyzed using the nonlinear regression curve fitting program GraphPad Prism 7 (GraphPad Software, Inc., San Diego, CA). From displacement assays at 25°C, the non-linear regression analysis for one site - Fit K_i was used to obtain logK_i values, which are provided by Prism by direct application of the Cheng-Prusoff equation:⁵⁵ $K_i = IC_{50} / (1 + ([L]/K_D))$ in which [L] is the exact concentration of [³H]CP55940 determined per experiment (i.e. ~1.5 nM). The kinetic K_D (1.24 ± 0.10 nM) of [³H]CP55940 was calculated using the formula $K_D = k_{off}/k_{on}$. The k_{on} (1.6 ± 0.1 × 10⁶ M⁻¹ s⁻¹) and k_{off} (2.0 ± 0.1 × 10⁻³ s⁻¹) of [³H]CP55940 at this temperature were determined using an association and dissociation assay, respectively (three experiments performed in duplicate). The logK_i values were converted manually to pK_i values (Table 1). For the kinetic experiments, a concentration equal to the IC₅₀ value of each agonist was used, as determined from the non-linear regression analysis for “one site - Fit logIC₅₀”. For non-linear regression analysis “one site - Fit K” and “one site - Fit logIC₅₀” the top and bottom of the curve were constrained at 100 and 0, respectively. From association assays, the association rate constant (k_{on}) of [³H]CP55940 was calculated using the formula $k_{on} = (k_{obs} - k_{off})/[L]$, in which [L] is the exact concentration of [³H]CP55940 determined per experiment. The observed association rate (k_{obs}) was determined with Prism’s “one-phase exponential association” analysis that uses the following formula: $Y = Y_0 + (Plateau - Y_0) * (1 - \exp(-k_{obs} * t))$, where Y₀ is the specific radioligand binding at time 0 (constrained at 0), Plateau represents the maximum specific [³H]CP55940 binding at equilibrium, k_{obs} is the observed association rate in min⁻¹ and t is the time in min. From dissociation assays, the dissociation rate constant (k_{off}) of [³H]CP55940 was determined using Prism’s “one-phase exponential decay” analysis using the following formula: $Y = (Y_0 - NSB) * \exp(-k_{off} * t) + NSB$, where k_{off} is the dissociation rate constant in min⁻¹ and where Y₀ is the specific radioligand binding at time 0 (constrained at 100). From competition association assays, the k_{on} and the k_{off} of cold ligands were obtained by non-linear regression analysis “kinetics of competitive binding” that uses the following equation:⁵⁶

$[RL] = Q * ((k_4 DIFF) / (K_F K_S)) + ((k_4 - K_F) / K_F) * \exp(-K_F t) - ((k_4 - K_S) / K_S) * \exp(-K_S t)$, using the following variables:

$$K_A = k_1 [L] (10^{-9}) + k_2$$

$$K_B = k_3 [I] (10^{-9}) + k_4$$

$$S = \sqrt{((K_A - K_B)^2 + 4 * k_1 k_3 [L] [I] (10^{-18}))}$$

$$K_F = 0.5 * (K_A + K_B + S)$$

$$K_S = 0.5 * (K_A + K_B - S)$$

$$DIFF = K_F - K_S$$

$$Q = (B_{max} k_1 [L] (10^{-9})) / DIFF$$

Where [RL] is the amount of receptor-ligand complex, [L] is the concentration [³H]CP55940 in nM per experiment (~1.5 nM), [I] depicts the used concentration of unlabeled competitor in nM, K_A and K_B are the observed association rates (k_{obs}) of [³H]CP55940 and the unlabeled competitor, respectively, k₁ and k₃ the association rate constants (k_{on} in M⁻¹min⁻¹) of [³H]CP55940 (determined per experiment) and the unlabeled competitor, respectively, k₂ and k₄ the dissociation rate constants (k_{off} in min⁻¹) of [³H]CP55940 (0.0115 min⁻¹, determined using three independent dissociation experiments) and the unlabeled competitor, respectively and t is the time in min. The k_{on} (M⁻¹min⁻¹) and k_{off} (min⁻¹) provided by Prism were converted manually to k_{on} (M⁻¹s⁻¹) and k_{off} (s⁻¹). Receptor residence time (RT, in min) was calculated by taking the reciprocal of the dissociation rate as follows room temperature = 1/(60*k_{off}), as k_{off} is in s⁻¹.

β-Arrestin recruitment and GTPγS data were analyzed by Prism’s nonlinear regression analysis “log (agonist) vs. response – variable slope” to obtain potency (EC₅₀) and efficacy (E_{max}) values of ligands. The efficacy of all agonists was normalized to the effects of 10 μM CP55940. The bottom of the curves were constrained at 0. All data was obtained from three separate experiments performed in duplicate, unless stated otherwise. The correlation between two independent variables or data sets was calculated using a two-tailed Pearson correlation analysis.⁵⁷ A P-value of less than 0.05 was considered significant.

References

1. Soethoudt, M.; Hoorens, M. W. H.; Doelman, W.; Martella, A.; Van der Stelt, M.; Heitman, L. H., Structure-kinetic relationship studies of cannabinoid CB2 receptor agonists reveal substituent-specific lipophilic effects on residence time. *Manuscript submitted*.
2. Zhang, R.; Monsma, F., Binding kinetics and mechanism of action: toward the discovery and development of better and best in class drugs. *Expert Opin Drug Discov* **2010**, *5*, (11), 1023-1029.
3. Copeland, R. A.; Pompliano, D. L.; Meek, T. D., Drug-target residence time and its implications for lead optimization. *Nat Rev Drug Discov* **2006**, *5*, (9), 730-739.
4. Lu, H.; England, K.; Ende, C. A.; Truglio, J. J.; Luckner, S.; Reddy, B. G.; Marlenee, N. L.; Knudson, S. E.; Knudson, D. L.; Bowen, R. A.; Kisker, C.; Slayden, R. A.; Tonge, P. J., Slow-Onset Inhibition of the FabI Enoyl Reductase from *Francisella tularensis*: Residence Time and in Vivo Activity. *ACS Chem Biol* **2009**, *4*, (3), 221-231.
5. Daryaei, F.; Chang, A.; Schiebel, J.; Lu, Y.; Zhang, Z.; Kapilashrami, K.; Walker, S. G.; Kisker, C.; Sotriffer, C. A.; Fisher, S. L.; Tonge, P. J., Correlating drug-target kinetics and in vivo pharmacodynamics: long residence time inhibitors of the FabI enoyl-ACP reductase. *Chem Sci* **2016**, *7*, (9), 5945-5954.
6. Gooljarsingh, L. T.; Fernandes, C.; Yan, K.; Zhang, H.; Grooms, M.; Johanson, K.; Sinnamon, R. H.; Kirkpatrick, R. B.; Kerrigan, J.; Lewis, T.; Arnone, M.; King, A. J.; Lai, Z.; Copeland, R. A.; Tummino, P. J., A biochemical rationale for the anticancer effects of Hsp90 inhibitors: slow, tight binding inhibition by geldanamycin and its analogues. *Proc Natl Acad Sci U S A* **2006**, *103*, (20), 7625-7630.
7. Copeland, R. A.; Williams, J. M.; Giannaras, J.; Nurnberg, S.; Covington, M.; Pinto, D.; Pick, S.; Trzaskos, J. M., Mechanism of selective inhibition of the inducible isoform of prostaglandin G/H synthase. *Proc Natl Acad Sci U S A* **1994**, *91*, (23), 11202-11206.
8. Copeland, R. A., The drug-target residence time model: a 10-year retrospective. *Nat Rev Drug Discov* **2016**, *15*, (2), 87-95.
9. Guo, D.; Hillger, J. M.; AP, I. J.; Heitman, L. H., Drug-target residence time—a case for G protein-coupled receptors. *Med Res Rev* **2014**, *34*, (4), 856-892.
10. Vauquelin, G.; Charlton, S. J., Long-lasting target binding and rebinding as mechanisms to prolong in vivo drug action. *Brit J Pharmacol* **2010**, *161*, (3), 488-508.
11. Cusack, K. P.; Wang, Y.; Hoemann, M. Z.; Marjanovic, J.; Heym, R. G.; Vasudevan, A., Design strategies to address kinetics of drug binding and residence time. *Bioorg Med Chem Lett* **2015**, *25*, (10), 2019-2027.
12. Van Aller, G. S.; Pappalardi, M. B.; Ott, H. M.; Diaz, E.; Brandt, M.; Schwartz, B. J.; Miller, W. H.; Dhanak, D.; McCabe, M. T.; Verma, S. K.; Creasy, C. L.; Tummino, P. J.; Kruger, R. G., Long residence time inhibition of EZH2 in activated polycomb repressive complex 2. *ACS Chem Biol* **2014**, *9*, (3), 622-629.
13. Dowling, M. R.; Charlton, S. J., Quantifying the association and dissociation rates of unlabelled antagonists at the muscarinic M3 receptor. *Br J Pharmacol* **2006**, *148*, (7), 927-937.
14. Vauquelin, G.; Bostoen, S.; Vanderheyden, P.; Seeman, P., Clozapine, atypical antipsychotics, and the benefits of fast-off D2 dopamine receptor antagonism. *Naunyn Schmiedebergs Arch Pharmacol* **2012**, *385*, (4), 337-372.
15. Sykes, D. A.; Moore, H.; Stott, L.; Holliday, N.; Javitch, J. A.; Lane, J. R.; Charlton, S. J., Extrapyramidal side effects of antipsychotics are linked to their association kinetics at dopamine D-2 receptors. *Nat Commun* **2017**, *8*, 763.
16. de Witte, W. E. A.; Danhof, M.; van der Graaf, P. H.; de Lange, E. C. M., In vivo Target Residence Time and Kinetic Selectivity: The Association Rate Constant as Determinant. *Trends Pharmacol Sci* **2016**, *37*, (10), 831-842.
17. Guo, D.; Mulder-Krieger, T.; AP, I. J.; Heitman, L. H., Functional efficacy of adenosine A(2)A receptor agonists is positively correlated to their receptor residence time. *Br J Pharmacol* **2012**, *166*, (6), 1846-1859.
18. Sykes, D. A.; Dowling, M. R.; Charlton, S. J., Exploring the mechanism of agonist efficacy: a relationship between efficacy and agonist dissociation rate at the muscarinic M3 receptor. *Mol Pharmacol* **2009**, *76*, (3), 543-551.
19. Tautermann, C. S.; Kiechle, T.; Seeliger, D.; Diehl, S.; Wex, E.; Banholzer, R.; Gantner, F.; Pieper, M. P.; Casarosa, P., Molecular Basis for the Long Duration of Action and Kinetic Selectivity of Tiotropium for the Muscarinic M3 Receptor. *J Med Chem* **2013**, *56*, (21), 8746-8756.

20. Ligresti, A.; De Petrocellis, L.; Di Marzo, V., From Phytocannabinoids to Cannabinoid Receptors and Endocannabinoids: Pleiotropic Physiological and Pathological Roles Through Complex Pharmacology. *Physiol Rev* **2016**, 96, (4), 1593-1659.
21. Mackie, K., Cannabinoid receptor homo- and heterodimerization. *Life Sci* **2005**, 77, (14), 1667-1673.
22. Mechoulam, R.; Hanus, L. O.; Pertwee, R.; Howlett, A. C., Early phytocannabinoid chemistry to endocannabinoids and beyond. *Nat Rev Neurosci* **2014**, 15, (11), 757-764.
23. Atwood, B. K.; Straiker, A.; Mackie, K., CB(2): therapeutic target-in-waiting. *Prog Neuropsychopharmacol Biol Psychiatry* **2012**, 38, (1), 16-20.
24. Galiegue, S.; Mary, S.; Marchand, J.; Dussossoy, D.; Carriere, D.; Carayon, P.; Bouaboula, M.; Shire, D.; Le Fur, G.; Casellas, P., Expression of central and peripheral cannabinoid receptors in human immune tissues and leukocyte subpopulations. *Eur J Biochem* **1995**, 232, (1), 54-61.
25. Pacher, P.; Mechoulam, R., Is lipid signaling through cannabinoid 2 receptors part of a protective system? *Prog Lipid Res* **2011**, 50, (2), 193-211.
26. Guindon, J.; Hohmann, A. G., Cannabinoid CB2 receptors: a therapeutic target for the treatment of inflammatory and neuropathic pain. *Br J Pharmacol* **2008**, 153, (2), 319-334.
27. Mukhopadhyay, P.; Baggelaar, M.; Erdelyi, K.; Cao, Z.; Cinar, R.; Fezza, F.; Ignatowska-Janlowska, B.; Wilkerson, J.; van Gils, N.; Hansen, T.; Ruben, M.; Soethoudt, M.; Heitman, L.; Kunos, G.; Maccarrone, M.; Lichtman, A.; Pacher, P.; Van der Stelt, M., The novel, orally available and peripherally restricted selective cannabinoid CB2 receptor agonist LEI-101 prevents cisplatin-induced nephrotoxicity. *Br J Pharmacol* **2016**, 173, (3), 446-458.
28. van der Stelt, M.; Cals, J.; Broeders-Josten, S.; Cottney, J.; van der Doelen, A. A.; Hermkens, M.; de Kimpe, V.; King, A.; Klomp, J.; Oosterom, J.; Pols-de Rooij, I.; de Roos, J.; van Tilborg, M.; Boyce, S.; Baker, J., Discovery and optimization of 1-(4-(pyridin-2-yl)benzyl)imidazolidine-2,4-dione derivatives as a novel class of selective cannabinoid CB2 receptor agonists. *J Med Chem* **2011**, 54, (20), 7350-7362.
29. Guo, D.; van Dorp, E. J.; Mulder-Krieger, T.; van Veldhoven, J. P.; Brussee, J.; IJzerman, A. P.; Heitman, L. H., Dual-point competition association assay: a fast and high-throughput kinetic screening method for assessing ligand-receptor binding kinetics. *J Biomol Screen* **2013**, 18, (3), 309-320.
30. Ostefeld, T.; Price, J.; Albanese, M.; Bullman, J.; Guillard, F.; Meyer, I.; Leeson, R.; Costantin, C.; Ziviani, L.; Nocini, P. F.; Milleri, S., A randomized, controlled study to investigate the analgesic efficacy of single doses of the cannabinoid receptor-2 agonist GW842166, ibuprofen or placebo in patients with acute pain following third molar tooth extraction. *Clin J Pain* **2011**, 27, (8), 668-676.
31. Soethoudt, M.; Grether, U.; Fingerle, J.; Grim, T. W.; Fezza, F.; de Petrocellis, L.; Ullmer, C.; Rothenhausler, B.; Perret, C.; van Gils, N.; Finlay, D.; MacDonald, C.; Chicca, A.; Gens, M. D.; Stuart, J.; de Vries, H.; Mastrangelo, N.; Xia, L.; Alachouzos, G.; Baggelaar, M. P.; Martella, A.; Mock, E. D.; Deng, H.; Heitman, L. H.; Connor, M.; Di Marzo, V.; Gertsch, J.; Lichtman, A. H.; Maccarrone, M.; Pacher, P.; Glass, M.; van der Stelt, M., Cannabinoid CB2 receptor ligand profiling reveals biased signalling and off-target activity. *Nat Commun* **2017**, 8, 13958.
32. Sykes, D. A.; Charlton, S. J., Slow receptor dissociation is not a key factor in the duration of action of inhaled long-acting ss(2)-adrenoceptor agonists. *Brit J Pharmacol* **2012**, 165, (8), 2672-2683.
33. Yu, Z.; van Veldhoven, J. P. D.; Louvel, J.; 't Hart, I. M. E.; Rook, M. B.; van der Heyden, M. A. G.; Heitman, L. H.; IJzerman, A. P., Structure-Affinity Relationships (SARs) and Structure-Kinetics Relationships (SKRs) of K(v)11.1 Blockers. *J Med Chem* **2015**, 58, (15), 5916-5929.
34. Miller, D. C.; Lunn, G.; Jones, P.; Sabnis, Y.; Davies, N. L.; Driscoll, P., Investigation of the effect of molecular properties on the binding kinetics of a ligand to its biological target. *Med Chem Comm* **2012**, 3, (4), 449-452.
35. Tresadern, G.; Bartolome, J. M.; Macdonald, G. J.; Langlois, X., Molecular properties affecting fast dissociation from the D2 receptor. *Bioorg Med Chem* **2011**, 19, (7), 2231-2241.
36. Guo, D.; Xia, L. Z.; van Veldhoven, J. P. D.; Hazeu, M.; Mocking, T.; Brussee, J.; IJzerman, A. P.; Heitman, L. H., Binding Kinetics of ZM241385 Derivatives at the Human Adenosine A(2A) Receptor. *Chem Med Chem* **2014**, 9, (4), 752-761.
37. Hua, T.; Vemuri, K.; Nikas, S. P.; Laprairie, R. B.; Wu, Y.; Qu, L.; Pu, M.; Korde, A.; Jiang, S.; Ho, J. H.; Han, G. W.; Ding, K.; Li, X.; Liu, H.; Hanson, M. A.; Zhao, S.; Bohn, L. M.; Makriyannis, A.; Stevens, R. C.; Liu, Z. J., Crystal structures of agonist-bound human cannabinoid receptor CB1. *Nature* **2017**, 547, (7664), 468-471.

38. Xia, L.; de Vries, H.; Lenselink, E. B.; Louvel, J.; Waring, M. J.; Cheng, L.; Pahlén, S.; Petersson, M. J.; Schell, P.; Olsson, R. I.; Heitman, L. H.; Sheppard, R. J.; IJzerman, A. P., Structure–Affinity Relationships and Structure–Kinetic Relationships of 1,2-Diarylimidazol-4-carboxamide Derivatives as Human Cannabinoid 1 Receptor Antagonists. *J Med Chem* **2017**, 60 (23), 9545–9564.
39. Zhang, R. D.; Hurst, D. P.; Barnett-Norris, J.; Reggio, P. H.; Song, Z. H., Cysteine 2.59(89) in the second transmembrane domain of human CB2 receptor is accessible within the ligand binding crevice: Evidence for possible CB2 deviation from a rhodopsin template. *Mol Pharmacol* **2005**, 68, (1), 69–83.
40. Griffin, G.; Atkinson, P. J.; Showalter, V. M.; Martin, B. R.; Abood, M. E., Evaluation of cannabinoid receptor agonists and antagonists using the guanosine-5'-O-(3-[S-35]thio)-triphosphate binding assay in rat cerebellar membranes. *J Pharmacol Exp Ther* **1998**, 285, (2), 553–560.
41. Louvel, J.; Guo, D.; Agliardi, M.; Mocking, T. A. M.; Kars, R.; Pham, T. P.; Xia, L. Z.; de Vries, H.; Brussee, J.; Heitman, L. H.; IJzerman, A. P., Agonists for the Adenosine A(1) Receptor with Tunable Residence Time. A Case for Nonribose 4-Amino-6-aryl-5-cyano-2-thiopyrimidines. *J Med Chem* **2014**, 57, (8), 3213–3222.
42. Martella, A.; Sijben, H.; Rufer, A.; Fingerle, J.; Grether, U.; Ullmer, C.; Hartung, T.; A, I. J.; van der Stelt, M.; Heitman, L., A novel selective inverse agonist of the CB2 receptor as a radiolabeled tool compound for kinetic binding studies. *Mol Pharmacol* **2017**, 92 (4), 389–400.
43. Nederpelt, I.; Bleeker, D.; Tuijt, B.; AP, I. J.; Heitman, L. H., Kinetic binding and activation profiles of endogenous tachykinins targeting the NK1 receptor. *Biochem Pharmacol* **2016**, 118, 88–95.
44. Nederpelt, I.; Kuzikov, M.; de Witte, W. E. A.; Schnider, P.; Tuijt, B.; Gul, S.; IJzerman, A. P.; de Lange, E. C. M.; Heitman, L. H., From receptor binding kinetics to signal transduction; a missing link in predicting in vivo drug-action. *Sci Rep-Uk* **2017**, 7 (1), 14169.
45. Xu, H. P.; Cheng, C. L.; Chen, M.; Manivannan, A.; Cabay, L.; Pertwee, R. G.; Coutts, A.; Forrester, J. V., Anti-inflammatory property of the cannabinoid receptor-2-selective agonist JWH-133 in a rodent model of autoimmune uveoretinitis. *J Leukocyte Biol* **2007**, 82, (3), 532–541.
46. Rajesh, M.; Pan, H.; Mukhopadhyay, P.; Batkai, S.; Osei-Hyiaman, D.; Hasko, G.; Liaudet, L.; Gao, B.; Pacher, P., Pivotal Advance: Cannabinoid-2 receptor agonist HU-308 protects against hepatic ischemia/reperfusion injury by attenuating oxidative stress, inflammatory response, and apoptosis. *J Leukocyte Biol* **2007**, 82, (6), 1382–1389.
47. Di Marzo, V., The endocannabinoid system: its general strategy of action, tools for its pharmacological manipulation and potential therapeutic exploitation. *Pharmacol Res* **2009**, 60, (2), 77–84.
48. Herring, A. C.; Koh, W. S.; Kaminski, N. E., Inhibition of the cyclic AMP signaling cascade and nuclear factor binding to CRE and kappa B elements by cannabinol, a minimally CNS-Active cannabinoid. *Biochem Pharmacol* **1998**, 55, (7), 1013–1023.
49. Eisenstein, T. K.; Meissler, J. J.; Wilson, Q.; Gaughan, J. P.; Adler, M. W., Anandamide and Delta(9)-tetrahydrocannabinol directly inhibit cells of the immune system via CB(2) receptors. *J Neuroimmunol* **2007**, 189, (1–2), 17–22.
50. Pandey, R.; Mousawy, K.; Nagarkatti, M.; Nagarkatti, P., Endocannabinoids and immune regulation. *Pharmacol Res* **2009**, 60, (2), 85–92.
51. Bot, I.; Ortiz Zacarias, N. V.; de Witte, W. E.; de Vries, H.; van Santbrink, P. J.; van der Velden, D.; Kroner, M. J.; van der Berg, D. J.; Stamos, D.; de Lange, E. C.; Kuiper, J.; AP, I. J.; Heitman, L. H., A novel CCR2 antagonist inhibits atherogenesis in apoE deficient mice by achieving high receptor occupancy. *Sci Rep* **2017**, 7, (1), 52.
52. Smith, P. K.; Krohn, R. I.; Hermanson, G. T.; Mallia, A. K.; Gartner, F. H.; Provenzano, M. D.; Fujimoto, E. K.; Goetze, N. M.; Olson, B. J.; Klenk, D. C., Measurement of protein using bicinchoninic acid. *Anal Biochem* **1985**, 150, (1), 76–85.
53. Harrison, C.; Traynor, J. R., The [35S]GTPgammaS binding assay: approaches and applications in pharmacology. *Life Sci* **2003**, 74, (4), 489–508.
54. Soethoudt, M.; van Gils, N.; van der Stelt, M.; Heitman, L. H., Protocol to Study beta-Arrestin Recruitment by CB1 and CB2 Cannabinoid Receptors. *Methods Mol Biol* **2016**, 1412, 103–111.
55. Cheng, Y.; Prusoff, W. H., Relationship between the inhibition constant (K1) and the concentration of inhibitor which causes 50 per cent inhibition (I50) of an enzymatic reaction. *Biochem Pharmacol* **1973**, 22, (23), 3099–3108.
56. Motulsky, H. J.; Mahan, L. C., The kinetics of competitive radioligand binding predicted by the law of mass action. *Mol Pharmacol* **1984**, 25, (1), 1–9.
57. Pearson, K., Determination of the Coefficient of Correlation. *Science* **1909**, 30, (757), 23–25.

